THESIS

CROSS-SCALE EVALUATION OF FUEL MAPS IN COLORADO PONDEROSA PINE-DOMINATED FORESTS

Submitted by

Katelyn J. Johnston

Department of Forest and Rangeland Stewardship

In partial fulfillment of the requirements

For the Degree of Master of Science

Colorado State University

Fort Collins, Colorado

Spring 2025

Master's Committee:

Advisor: Chad Hoffman
Co-Advisor: Wade Tinkham

Todd Hawbaker
Jody Vogeler

ABSTRACT

CROSS-SCALE EVALUATION OF FUEL MAPS IN COLORADO PONDEROSA PINE-DOMINATED FORESTS

Fuel maps are used in every aspect of wildfire management, allowing managers to assess fire risk, predict fire behavior and effects, and guide fuel hazard treatment planning. Despite widespread use of national fuel maps like LANDFIRE, FCCS, and FastFuels, quantitative data on their accuracy and biases across ecosystems and scales remain limited. The few studies evaluating LANDFIRE's canopy fuel maps and FCCS have identified a wide range of errors and conflicting bias trends. Additionally, LANDFIRE's 40 standard fire behavior fuel models have yet to be assessed for their ability to represent fuel component loadings, despite growing use in fuel maps like FastFuels for physics-based fire behavior modeling. The accuracy of FastFuels has not been evaluated due to its recent development. The overall objective of this study was to assess the accuracy and bias of three national fuel mapping products – LANDFIRE, FCCS, and FastFuels – at five different scales. To meet this objective, I sampled surface and canopy fuels from seven sites representing the range of ponderosa pine (*Pinus ponderosa* Dougl. Ex Laws.) fuel complexes across the Colorado Front Range. Plots at each site were arranged in a 5x5 grid of 0.09 ha pixels to allow for accuracy assessment at 0.09, 0.12, 0.81, 1.44, and 2.25 ha scales. My results indicate that all three national fuel mapping products performed poorly across fuel attributes, with systematic biases and mean absolute errors ranging from 36% to 2590%. Errors and biases associated with LANDFIRE canopy metrics suggest that LANDFIRE is likely to overestimate fuel hazards associated with crown fire initiation, but underestimate crown fire spread hazard, while FastFuels underestimates the hazards

associated with both crown fire initiation and spread. Similarly, FBFM40 overestimates key surface fuel components, such as fine fuel loading, which would likely lead to overpredicted surface fire behavior. FCCS metrics crucial for smoke and emissions forecasting, particularly 1000-hour fuels, are also overestimated, potentially inflating emissions projections. I found no significant relationship between mean error and map scale from 0.09 ha to 2.25 ha. The variation observed within and between fuel components and layers of LANDFIRE, FCCS, and FastFuels highlights inherent challenges associated with mapping wildland fuels. The high errors and biases observed in my assessment may have broader implications for fire management and planning, warranting further investigation, as these fuels play an important role in dictating fire behavior and effects. Although advancements in remote sensing and modeling offer opportunities to improve these national fuel mapping products, uncertainties in current products should continue to be quantified and considered when implemented in management activities until these improvements are successfully integrated.

ACKNOWLEDGEMENTS

The last few years in this program have been filled with challenges, friendship, laughter, and growth, and I have endless gratitude for everyone who has supported me along the way.

First and foremost, I would like to thank my advisor, Chad Hoffman, for his patience and support in guiding me through this process. His expertise in fire science and modeling, along with his experience as an advisor, is evident, and I am grateful for the insight and opportunities he has provided. Thanks to my co-advisor, Wade Tinkham, who has provided guidance in every aspect of this project – from statistical analysis and technological troubleshooting to writing support – all while somehow finding time to help with extensive fieldwork despite his busy schedule. I also extend my sincere appreciation to the other members of my committee: Todd Hawbaker and Jody Vogeler, for their invaluable guidance in study design and remote sensing. Their insightful feedback has played a crucial role in shaping this research, and I am grateful for their time and expertise.

I was incredibly fortunate to have fantastic field technicians (Rick Grybko, Lydia Hoffman, Rylee Aksamit, Max Pohl, and Parker Neal) who kept long, tedious field days fun and productive.

I would also like to thank Boulder and Jefferson County land managers for their assistance in site selection and access and to thank my funding source: SERDP grant RC19-1119.

To my fellow graduate 'cohort': I cannot thank you enough for the camaraderie, direction, and much-needed distractions throughout this journey. I have learned so much from each of you, and I am incredibly grateful for the community we have built and for the office tomfoolery, including the quote board. *"Why wrangle data when I can wrangle horses?" – Kate Johnston, probably (Lad, 2024)*

Thank you to the Gunne(a)rs that have been by my side throughout the entirety of this process, for providing support and laughter, and for helping maintain my physical and mental well-being through countless runs and outings to the Poudre River, Horsetooth Reservoir, and breweries.

To my partner, Danny – thank you for your relentless support, patience, and compassion. Your ability to mitigate stress with exceptional home-cooked meals, gin rummy, and laughter has been crucial. Thank you to my friends from afar, especially Emily and Zach Forcade, for always providing me with adventures to look forward to and the many hours of check-in calls. And thank you to the incredible community of rec soccer folks that have taken me in as a member of the family for providing an athletic outlet, but also for supporting me in every endeavor – I am endlessly grateful for this army of people that I can count on for anything at any time.

Finally, thank my parents for always believing in me, inspiring me to set high standards and achieve my goals, and fostering my love for natural resources. Your hours spent reviewing drafts, redirecting stress, and providing encouragement have been invaluable.

TABLE OF CONTENTS

CROSS-SCALE EVALUATION OF FUEL MAPS IN COLORADO PONDEROSA PINE-DOMINATED FORESTS

1. INTRODUCTION

Wildland fuels are a critical factor in wildfire management and planning as they are the only variable in the fire behavior triangle (i.e., topography, weather, and fuels) that can be directly manipulated and managed (Agee, 1996; Countryman, 1972; Keane et al., 2001; Loudermilk et al., 2017; Lydersen et al., 2017; Pierce et al., 2009). The relationship between fuel loading, composition and arrangement, and fire behavior provides the basis for assessments of fire risk (Ager et al., 2011; Chuvieco et al., 1997; Gouma and Chronopoulou-Sereli, 1998), fuel hazard treatment planning (Chuvieco and Congalton, 1989; Ottmar et al., 2012; Thompson et al., 2022), forecasts of smoke and emissions (Larkin et al., 2014; Liu et al., 2019), predictions of fire effects (Atchley et al., 2021; Dos Santos et al., 2021), and prescribed fire planning (Duff et al., 2019; Gould et al., 2023). Managers often rely on fuel maps to provide spatial data for use in many of these applications; however, accurately representing the distribution and loading of wildland fuels is difficult due to their remarkable spatial and temporal variability (Keane et al., 2001; Vakili et al., 2016). Given the time and effort required to measure variability in wildland fuels, few studies have evaluated how well current fuel maps capture this variability within the fuels complex – a crucial factor influencing the accuracy of fire management and planning tools.

To simplify the complexity associated with the fuels complex, wildland fuels are classified into three vertical strata - ground, surface, and canopy (Keane, 2015). These strata are further delineated into individual fuel components whose properties govern fire ignition, spread, and intensity (Anderson, 1982; Scott and Burgan, 2005). Ground fuels occupy space between the

mineral soil layer and the litter layer, including components such as duff, peat, and buried roots (Hu et al., 2018; Keane, 2015; Nelson Jr., 2001). Although ground fuels are not often associated with active fire behavior at the flame front and are therefore not considered in fire behavior modeling, they are important components related to smoke emissions (Che Azmi et al., 2021; Hungerford et al., 1995; Ottmar, 2014) and tree and soil biota mortality from soil heating and smoldering (Kreye et al., 2020; Varner et al., 2007). Surface fuel components include combustible biomass scattered on or growing near the ground surface, such as litter, downed dead woody debris, herbaceous and woody vegetation, and small trees (Brown and See, 1981; Burgan and Rothermel, 1984). Surface fuels influence fire behavior by providing the substrate that supports fire spread and the radiative and convective heating that can scorch overstory trees or allow surface fires to transition into the canopy fuel layer (Hall and Burke, 2006; Scott and Reinhardt, 2001). Canopy fuels are combustible biomass associated with shrub and tree biomass above two meters from the ground (Van Wagner, 1977; Rothermel, 1991). Attributes of canopy fuels, such as canopy bulk density, base height, and cover are important factors contributing to the likelihood of crown fire initiation and spread (Hall and Burke, 2006).

Traditionally, land managers have relied on a combination of direct and indirect field sampling methodologies to produce stand-level (10-100s ha) estimates of various surface and canopy fuel metrics. The surface fuel complex is most commonly described by the fuel loading (kg m^{-2}) of individual fuel components (e.g., 1-, 10-, 100-, and 1000-hour dead and down woody debris, herbaceous and shrub fuels) which are critical inputs for most fire behavior and effects models (Arroyo et al., 2008; Burgan, 1987; DeCastro et al., 2022; Finney, 1998; Keane, 2015; Linn et al, 2020). At the most basic level, estimates for surface fuel loads can be made using destructive sampling methods where fuels are collected from fixed or variable radius plots, dried in the laboratory, and weighed. Although this method is widely regarded as the most accurate and

unbiased estimate of fuel loading (Keane and Gray, 2013) and is often used to provide reference data in validations of other sampling techniques (Hudak et al., 2020; Reinhardt et al., 2006; Rowell et al., 2020; Tinkham et al., 2015; Volkova et al., 2016), its application across large spatial scales is unrealistic due to the significant time and effort required (Sikkink and Keane, 2008). Indirect methods such as planar-intersect surveys (Brown, 1974), where intercepts of fuel particles are tallied and converted to a fuel load, and ocular estimates such as the photoload (Keane and Dickinson, 2007) and photo series (Ottmar and Vihnanek., 1998) approaches are also popular surface fuel inventory approaches. Of these methods, planar intersect surveys are the most commonly employed method to estimate fine and coarse woody debris fuel loading but also require substantial sampling effort (Lutes et al., 2006; Waddell, 2002). In an evaluation comparing these surface loading estimates, Sikkink and Keane (2008) determined that 250 to 750 m of transect line per 1 kg m^{-2} of fuel load was necessary to estimate fine and coarse woody debris in a fixed 2500 m^2 plot, requiring field crews up to 45 minutes to complete the work. Photoload estimates, which involve ocular estimation of observed fuelbed conditions from reference photos depicting increasing fuel loads, and photo series, a similar approach used for larger scales, require surveyors to walk through the unit and match conditions with reference photos (Keane and Dickinson, 2007; Sandberg et al., 2001). Both methods are considerably more efficient than destructive sampling or planar intersect, often taking less than ten minutes per plot (Sikkink and Keane, 2008). However, they tend to be less accurate (Keane and Gray, 2013), frequently overestimating low fuel and underestimating high fuel loads, though errors can be corrected using double sampling approaches (Tinkham et al., 2015).

Descriptions of the canopy fuel complex often emphasize estimates of canopy fuel load (kg m^{-2}), bulk density (kg m^{-3}), and base height (m), as these variables are critical inputs for the prediction of the initiation, spread, and intensity of crown fire (Albini 1996; Andrews et al., 2005; Cruz et al.,

2005; Finney 1998; Van Wagner 1977; Rothermel 1991). In the western US, land managers commonly estimate canopy fuel load and canopy bulk density indirectly using forest inventory data and associated allometric equations that relate tree properties (i.e., species, diameter at breast height, crown ratio) to biomass (Brown 1978; Brown et al., 1989; Chave et al., 2005; Chave et al., 2014). Individual tree estimates are then scaled up to represent stand-level metrics. Previous studies have indicated that biomass estimates from allometric equations, like those defined by Brown (1978), Brown et al. (1989), Chave et al. (2005), and Chave et al. (2014) can be modified to include locally derived relationships to improve accuracy and correlation (Walker et al., 2016). For example, Reinhardt et al. (2006), observed decreases of 64% and 50% in bias when comparing canopy bulk density and canopy fuel load estimates from non-adjusted to locally adjusted allometric equations. Although modified allometric equations tend to produce higher accuracy than other methods, collecting the necessary data (often through destructive sampling or remote sensing) to derive relationships between attributes such as tree diameter, wood density, and above-ground biomass can be time-consuming and expensive (Djomo and Chimi, 2017; Pimont et al., 2015). Canopy fuel load and bulk density can also be estimated using stand-scale allometric equations with common stand descriptors (e.g., stand density, basal area, stand height) as the dependent variables (Cruz et al., 2003; Ruiz-González and Álvarez-González, 2011).

Although land managers have successfully employed various field sampling-based methods for fuel monitoring and management, these approaches are often time-consuming and costly, making them impractical for creating the necessary fuel maps to support spatial fire behavior modeling, wildfire risk assessments, landscape-scale planning, and the development of treatment strategies (Keane and Dickinson, 2007). Instead, the development of most fuel maps involves a standardized process that integrates field and auxiliary data to generate maps of specified resolutions and extents. This process is typically accomplished by collecting field inventory data from a subset of

points within the target area(s). Next, a model of a fuel metric of interest (e.g., surface fuel load or canopy bulk density) is developed using a spatial interpolation method to produce estimates at unsampled locations (Hoffman et al., 2023). Common approaches for development of fuel maps include classification (Domingo et al., 2020; McKenzie et al., 2007; Ottmar et al., 2007; Shaik et al., 2021), regression (Krasnow et al., 2009; Peterson et al., 2008; Reeves et al., 2009), and geostatistical methods such as kriging (Lin et al., 2021; Pierce et al., 2009). The accuracy, resolution, and extent of the resultant fuel map are dictated by the sampling scheme (both to collect field inventory and auxiliary data) and the spatial interpolation method selected.

Remotely sensed data is increasingly being utilized to support fuel mapping efforts because it can capture snapshots of landscape fuel conditions across a range of spatial and temporal resolutions and extents (Chuvieco, 2020; Keane et al., 2001; Rollins et al., 2004; Szpakoski and Jensen, 2019; Vogeler et al., 2016; Wooster et al., 2021). For example, terrestrial Light Detection and Ranging (LiDAR) systems (TLS) have been used to produce fuel maps at sub-meter resolutions, while satellite imagery from Landsat supports national-scale fuel mapping at a 30 m resolution, and Moderate Resolution Imaging Spectroradiometer (MODIS) offers coarse-scale maps with spatial resolutions of 250, 500, and 1,000 m. The drawbacks and benefits associated with fuel maps derived from remotely sensed data relate to the selected sensor. For instance, TLS can capture fine-scale variability (Donager et al., 2021; Hudak et al., 2020; Loudermilk et al., 2007), but its spatial extent is constrained by the laser's range, which often limits point cloud capture to well less than the 150 m often quoted by manufactures for engineering applications (Stovall et al., 2021). Additionally, while TLS has proven effective in some ecosystems (e.g., surface fuel characterization in Southeastern U.S. pine systems; Loudermilk et al., 2023), its broader application remains limited by the need for extensive validation datasets and technical challenges such as occlusion (Åkerblom and Kaitaniemi, 2021; Donager et al., 2021). Broad-scale maps, like

those derived from Landsat, the Sentinel satellites, or MODIS often struggle to capture fine-scale variability at scales of 1-10 m because they generalize fuel attributes into broad map units (e.g., 30 m pixels). Additionally, because satellite-based passive remote sensing data is captured from above the canopy, they often fail to capture the variability of surface fuels, which become obstructed by the canopy (Rollins et al., 2004).

Given the wide range of spatial resolutions available to remote sensors, fuel maps can be produced across different scales and resolutions to address management objectives (Figure 1.1). For instance, fine-scale fuel maps, which can be used for prescribed fire planning (Keane and Reeves, 2011), do not capture the broad-scale fuel complex information necessary for many other management and planning tasks, such as forecasting smoke and emissions from large wildfires (Marsha and Larkin, 2022). Similarly, while local- and regional-scale fuel maps may better represent the fine-scale variability of fuels than national fuel maps, they are often developed using inconsistent methodologies, resulting in cross-boundary incompatibility (Keane et al., 2001). This inconsistency poses a significant problem for broad-scale wildfire management and planning that spans geographic and managerial bounds. The need for spatially continuous, consistent fuel maps that provide the necessary inputs for fire management and planning tools leads many managers to rely on national-scale fuel maps such as the Landscape Fire and Resource Planning Tools (LANDFIRE; Reeves et al., 2009), the Fuel Characteristic Classification System (FCCS; Ottmar et al., 2003; Ottmar et al., 2007; Riccardi et al., 2007), and FastFuels (Marcozzi et al., 2024).

LANDFIRE is the most widely used national mapping product in the US, consisting of over twenty-five geospatial layers, with thirteen different fuel variables that are used by land managers for quantifying fuel hazard, assessing wildfire risk, and predicting fire behavior and effects. LANDFIRE fuel maps are developed by combining satellite imagery, biophysical gradients (e.g., temperature, humidity, slope, aspect, etc.), and vegetation structure and composition (i.e.,

dominant ecological system, dominant life form, and average height) to map vegetation, fuels, disturbance regimes, historical fire regimes, and topography as a 30 m rasterized grid across the coterminous United States (Reeves et al., 2009). Many of LANDFIRE's fuel layers build upon vegetation layers including existing vegetation type, existing vegetation cover, existing vegetation height, and environmental site potential (LANDFIRE, 2020; 2023a; 2023b; 2023c; 2023d; 2023e; 2023f; 2023g). These vegetation layers are developed by utilizing training data from field assessment and LiDAR observations, then combined with Landsat imagery to inform models that assign vegetation components (LANDFIRE, 2023b; 2023c; 2023d).

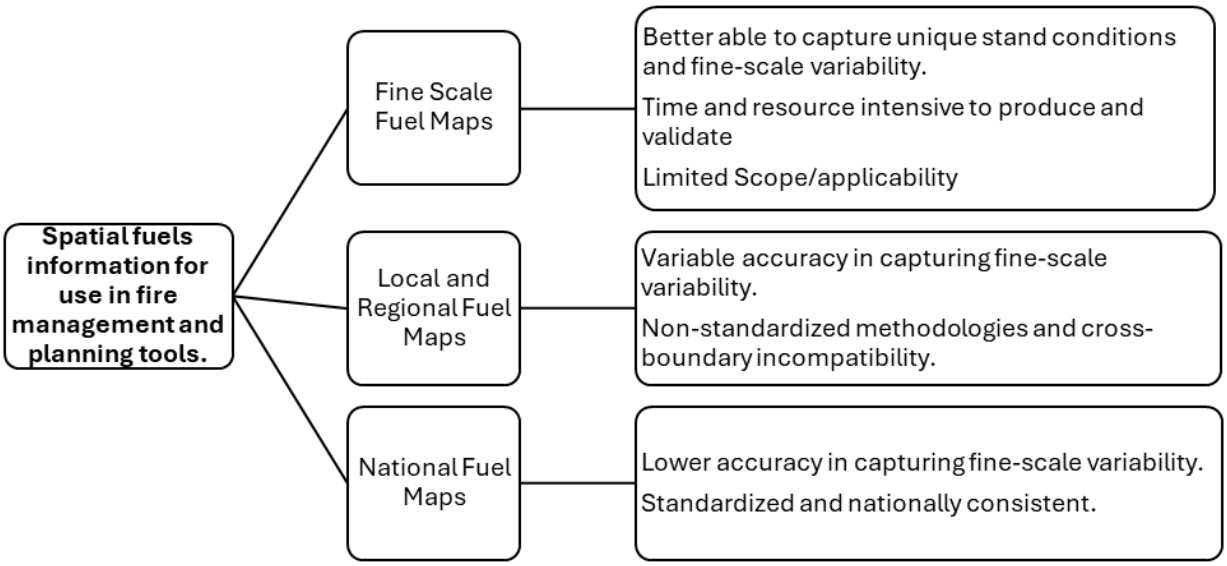

Figure 1.1. Flow chart relating fuel loading map scale with corresponding benefits and drawbacks.

LANDFIRE reports surface fuel characteristics as two sets of standard fire behavior fuel models: the Anderson (1982) 13 standard fire behavior fuel models (FBFM13) and the Scott and Burgan (2005) 40 standard fire behavior fuel models (FBFM40). FBFM's provide the necessary simplified descriptions of surface fuels used in fire behavior and effects models based on Rothermel (1972). The FBFM40 fuel models have been incorporated into other fuel mapping tools such as FastFuels (Marcozzi et al., 2024). The FBFM40 are grouped by fire-carrying fuel type, and

were developed from a compilation of fuels complex information from the Natural Fuels Photo Series (Ottmar and Vihnanek, 1998, 1999, 2000, 2002; Ottmar et al., 1998, 2000a, 2000b, 2002, 2003b; Wright et al., 2002) and were assigned to capture the range of common fuel conditions encountered in fire management and planning (Scott and Burgan, 2005). LANDFIRE assigns fuel models to the 30 m raster using rulesets based on the LANDFIRE vegetation layers that were calibrated and reviewed by local experts (Reeves et al., 2009). Canopy fuel complex loads and attributes are also reported by LANDFIRE at a 30 m resolution. These canopy map layers are also developed from spatial interpolation methods using the LANDFIRE vegetation layers, US Forest Service Forest Inventory and Analysis (FIA) field referenced data, and remotely sensed data from Landsat to model, estimate, and report canopy height, cover, bulk density, and base height (LANDFIRE, 2023e; 2023f; 2023g).

FCCS fuelbeds, which were designed independently of LANDFIRE (Ottmar et al., 2007; Riccardi et al., 2007a), provide estimates of wildland fuels for six strata: canopy, shrubs, nonwoody fuels, woody fuels, litter-lichen-moss, and ground fuels. Currently, there are 216 FCCS fuelbeds organized across a range of ecoregions, vegetation forms, structural classes, cover types, change agents, natural fire regimes, and fire regime condition classes (McKenzie et al., 2007; Ottmar et al., 2007). These fuelbeds represent fuels complexes as homogeneous units according to distinct combustion environments, focusing specifically on variables that are important for fuels management and fire behavior planning (Riccardi et al., 2007b). FCCS fuel beds have been interpolated on the same 30 m raster as LANDFIRE using a rule-based crosswalk between the fuelbed and the LANDFIRE existing vegetation layer (LANDFIRE, 2020; 2023g). The FCCS fuelbeds were organized using ecoregion, vegetation form, structural class, cover type, change agent, natural fire regime, and fire regime condition class. These fuelbeds represent fuels complexes as homogeneous units

according to distinct combustion environments, focusing specifically on variables that are important for fuels management and predicting fire behavior (Riccardi et al., 2007b).

FastFuels (Marcozzi et al., 2024) is a fuels mapping product that provides 3D fuels data for use in advanced physics-based 3D fire models such as QUIC-Fire (Linn, 2020) and the Wildland-Urban Interface Fire Dynamics Simulator (WFDS; Mell et al., 2007; Mell et al., 2010). FastFuels leverages rasterized predictions of forest inventory plots from TreeMap (Riley et al., 2021) and surface fuels data from LANDFIRE's FBFM40 combined with remote sensing imagery from Sentinel-2 and Landsat satellites and statistical and machine learning techniques to transform 2D fuels information from 30 m resolutions to a continuous rasterized grid of sub-meter resolution fuels data (Marcozzi et al., 2024). TreeMap, which was originally developed for carbon mapping, uses random forest models, forest inventory data, and spatial data from LANDFIRE to compile a list of trees over 2.5 cm diameter at breast height and common stand metrics for trees over 2.5 cm diameter at breast height (e.g., trees per acre, basal area, quadratic mean diameter) within a 30 m pixel (Riley et al., 2022). TreeMap's tree lists include tree species, height, diameter, and live or dead status for each tree. FastFuels imputes each 30 m resolution tree list and assigns exact tree locations using a Poisson point process (Marcozzi et al., 2024). An advantage of the FastFuels data structure is that users can scale canopy fuels from individual tree observations to coarser rasterized datasets allowing the data's use in traditional rasterized fire models like BehavePlus, FlamMap, and FARSITE (Andrews, 2013; Finney, 2006; Finney, 1998), but also physics-based models requiring tree-level inputs like WFDS, FIRETEC, and QUIC-Fire (Linn, 2020; Linn et al., 2002; Mell et al., 2007; Mell et al., 2010).

Despite widespread use of surface and canopy fuel maps, previous assessments of their accuracy and bias are lacking in many ecosystems or have reported high errors (up to 200%), with conflicting results on over- and under-predictions of certain fuel components (Hyde et al., 2015;

Keane et al., 2013; McCarley et al., 2022). For example, Hyde et al. (2015) sampled 0.04 ha plots in mixed conifer forests of Idaho and found that FCCS fuel loadings underrepresented litter and 10- and 100-hour fuels, while overrepresenting duff and herbaceous loadings. In contrast, Keane et al. (2013), who compared FCCS fuelbed loadings with FIA data from 0.06 ha plots of varying forest types across eight states in the western United States, found that FCCS underpredicted all surface fuel components. To my knowledge, there are no assessments of fuel loadings predicted by FBFM40 fuel models as these approaches were originally designed for modeling fire behavior using the Rothermel (1972) model and are not assumed to represent actual fuel loadings on the ground. Evaluation of their effectiveness at predicting fire behavior can be found in Forghani et al. (2007), Krasnow et al. (2009), and Price and Germino (2022). Given that FBFM40 are being used to represent actual fuel loads for use in physics-based models (Marcozzi et al., 2024), there is a critical need for a fuel load-focused evaluation.

Evaluations of canopy fuel layer maps show more consistent results than those for the surface fuel layer. Reeves et al. (2009) observed that LANDFIRE overpredicted canopy base height (CBH) and canopy cover (CC), and underpredicted and crown bulk density (CBD) values compared to measured canopy metrics from plots (mostly 0.06 ha FIA plots) across the United States. Krasnow et al. (2009) conducted a complete tree census of 0.01-0.09 ha plots in a mixed conifer region of the Colorado Front Range, also finding that LANDFIRE overpredicted CBH and CC, and underpredicted CBD. Although FastFuels has not been extensively evaluated, assessments of TreeMap have shown accuracy rates from 57% to 87.4% in matching canopy cover and disturbance codes, respectively (Riley et al., 2022). Further evaluation is needed to determine how errors associated with TreeMap translate into the accuracy of FastFuels mapping.

In addition to the limited comprehensive studies evaluating fuel map accuracies, there are no evaluations of the effect of spatial scale on fuel map accuracy. Previous assessments of national

fuel maps have focused on single-pixel (0.09 ha) comparisons. However, the accuracy of these fuel maps could be affected at larger scales due to the spatial autocorrelation of individual fuel components and the broad-scale data used in the development of these products. For example, most canopy fuel attributes exhibit variability beyond the 30 m resolution of most national fuel maps (e.g., CBD semivariance ranging from 100 to 440 m, Keane et al., 2012). Though the effects of spatial scale have not been investigated for wildland fuels, studies from other areas of forest mapping show mixed results. For example, Sprintisin et al. (2007) found that maps with 4 m and 250 m resolutions produced similar outcomes when assessing the spatial distribution of leaf area index in forest stands. Conversely, in a study identifying forest cover from satellite data, Salajanu and Olson Jr. (2001) emphasized that finer map resolutions are crucial to drawing meaningful conclusions. Understanding the role of spatial scale on fuel map accuracy could provide further insight into fuel map limitations and help improve the appropriate use of these tools in fire management and planning.

Comprehensive evaluation of national fuel mapping products such as LANDFIRE, FCCS, and FastFuels is crucial, given their widespread use in support of many critical fire management and planning tools. Outputs from these fuel maps that differ substantially from actual fuel loads could cause misleading predictions of fire behavior and effects, jeopardizing lives, infrastructure, and natural resources. To address these challenges, this study (1) evaluates LANDFIRE, FCCS, and FastFuels for accuracy for surface and canopy fuels and (2) assesses how increasing map scales affect the accuracy of those fuel maps. By evaluating these three fuel mapping data products through a side-by-side comparison, this study provides valuable guidance for managers to make informed decisions about selecting fuel maps tailored to specific objectives.

2. METHODS

2.1. Study area

To evaluate surface and canopy fuel estimates from LANDFIRE, FCCS, and FastFuels I selected seven sites across the Colorado Front Range of the interior western United States. The seven sites were chosen to represent a wide range of ponderosa pine-dominated forests in the region, including long untreated forests as well as those that received fuel hazard reduction treatments or were impacted by severe wildfire or insect outbreaks (Table 1.1). These sites were chosen in consultation with regional US Forest Service personnel and Boulder and Jefferson County land managers to best reflect the range of forest structures and disturbance histories they oversee (Figure 1.2).

Colorado Front Range ponderosa pine-dominated (*Pinus ponderosa Dougl. ex Laws.*) forests have been chosen as the focal ecosystem for this study. Ponderosa pine is the most widely distributed pine species in North America (Oliver and Ryker, 1990), making it an ideal subject for generating more broadly applicable findings. Additionally, ponderosa pine dominates many wildland-urban-interface (WUI) regions, a key area of management concern due to its rapid expansion, particularly in Colorado where the WUI is among the fastest growing in the country (Merschel et al., 2021; Theobald and Romme, 2007). The Colorado Front Range, in particular, has been identified by the U.S. Forest Service as a high-risk fireshed, where environmental conditions and increased community exposure have led to its selection as one of the twenty-one Wildfire Crisis Strategy landscapes for understanding wildfire behavior and improving fuel management (USDA Forest Service, 2022). Given the vulnerability of this ecosystem and the communities it surrounds, accurate fuel mapping is essential to support wildfire risk assessments and the design of proactive land management treatments to reduce the negative impacts of future wildfires.

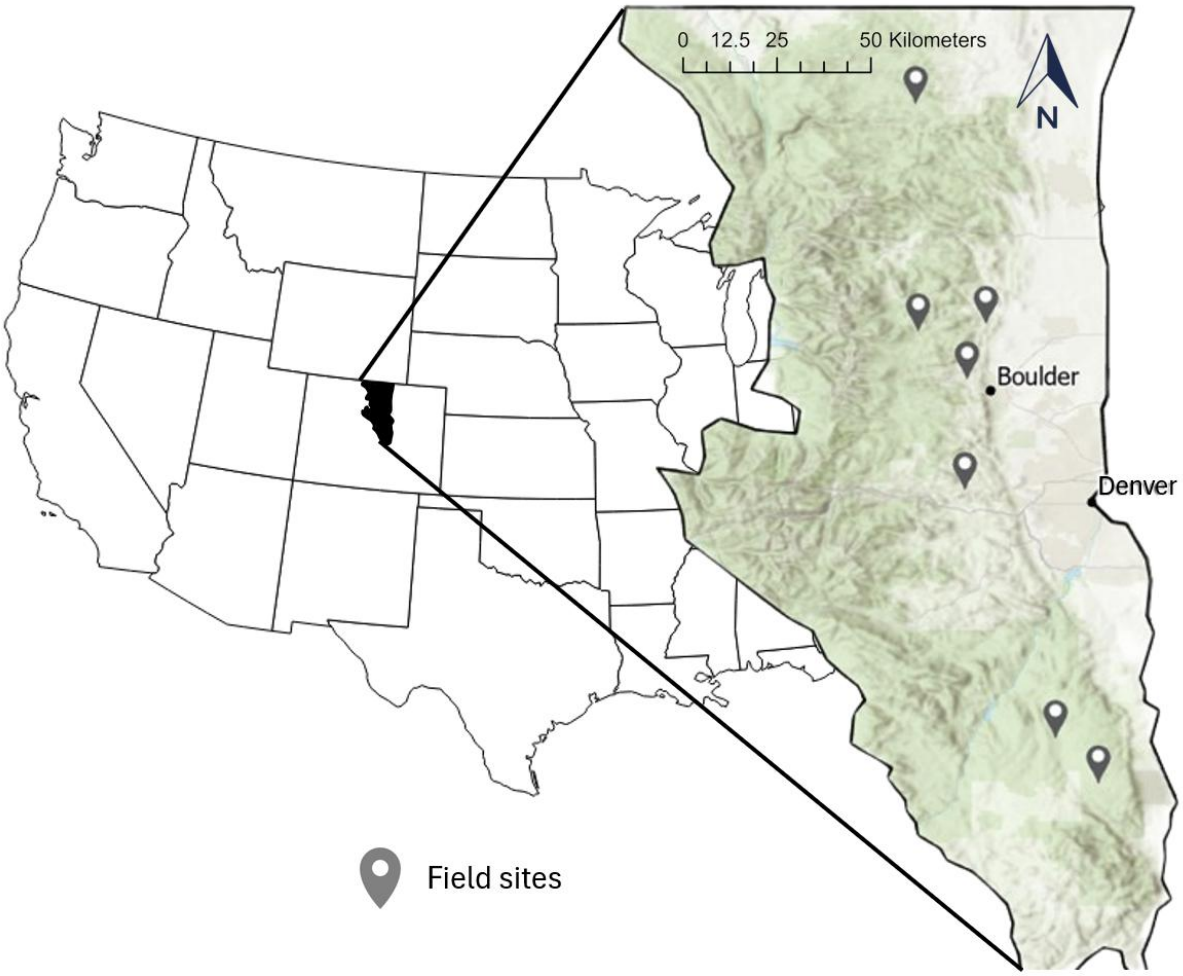

Figure 1.2. Map of field sites ordered latitudinally from north to south, Ben Delatour Scout Ranch, Heil Valley Ranch, Bunce School Road (Wallace property), Bald Mountain Scenic Area, Centennial Cone Park, Manitou Experimental Forest (N1), Pikes Peak Forest Dynamics Plot.

Table 1.1. Sample locations – ordered latitudinally from north to south across the Colorado Front Range. Site elevation, slope, and aspect represent the average of individual sampling plots. Untreated indicates no recent treatment or severe insect or fire-caused tree mortality.

Site	County	Elevation (m)	Aspect	Slope (%)	Treatment History
Ben Delatour Scout Ranch	Larimer	2292	NE	25	Untreated
Heil-Valley Ranch	Boulder	1999	E	18	Untreated
Bunce School Road (Wallace)	Boulder	2494	NE	13	Untreated
Bald Mountain Scenic Area	Boulder	2067	SE	23	2008 thin, pile burns, and broadcast burn
Centennial Cone Park	Jefferson	2361	NW	25	Untreated
Manitou Experimental Forest (N1)	Teller	2354	NE	7	Untreated
Pikes Peak Forest Dynamics Plot	El Paso	2794	SW	21	2020 thin w/pile burns

The sites stretch across five counties and are located between approximately 39°N to 40°N latitude at -105°W longitude, with elevations ranging from 2000 to 2800 meters. Slopes varied across and within sites, ranging from 7% to 25%. From 1990 to 2020, sites received an average of 43.6 to 63.5 cm of precipitation annually (PRISM Climate Group, 2024). Precipitation peaks occurred during spring rain/snow showers (March to May) and again in late summer due to monsoonal thunderstorms (July to August). Thirty-year (1990-2020) average annual and maximum temperatures at the sites ranged from 4.4 to 9.4 C°, with maximum and minimum temperatures of 11.5 to 16.3 C° and -2.7 to 2.5 C° occurring in July and December through February, respectively. Ponderosa pine was the dominant overstory tree species of all sites, with minor components of Douglas-fir (*Psuedotsuga menziesii* (Mirb.) Franco), Engelmann spruce (*Picea engelmannii* Parry ex Engelm.), quaking aspen (*Populus tremuloides* Michx.), Rocky Mountain juniper (*Juniperus scopulorum* Sarg.), and limber pine (*Pinus flexilis* James). Understory conditions varied within and between sites, ranging between productive, moist conditions with dense herbaceous and woody vegetation and dense regrowth (Figure 1.3, d & g), to dry, open, parklike stands with high volumes of needle litter and limited herbaceous and woody vegetation and regeneration (Figure 1.3, b & e).

2.2. Field methods

Forest and fuel inventory methods were selected to mimic the field protocols underpinning the LANDFIRE, FCCS, and FastFuels national mapping products. On each site, a single 150 m x 150 m plot was randomly established and divided into a 5x5 grid of 30 m x 30 m (0.09 ha) pixels (Figure 1.4). Thirteen 0.04 ha circular subplots were established from the center points of alternating pixels. In each subplot, species, height, CBH, crown class, and diameter at breast height (DBH) were recorded for all trees with a DBH ≥ 12.7 cm. To measure trees with a DBH below 12.7 cm, a 13 m^2 circular microplot was established 3.7 m from subplot center at an azimuth of 330 degrees. The

DBH, species, and height of seedlings (DBH < 2.54 cm, height > 0.15 m tall for conifers and 0.30 m tall for hardwoods) and saplings (DBH 2.54-12.69 cm) were recorded within each microplot.

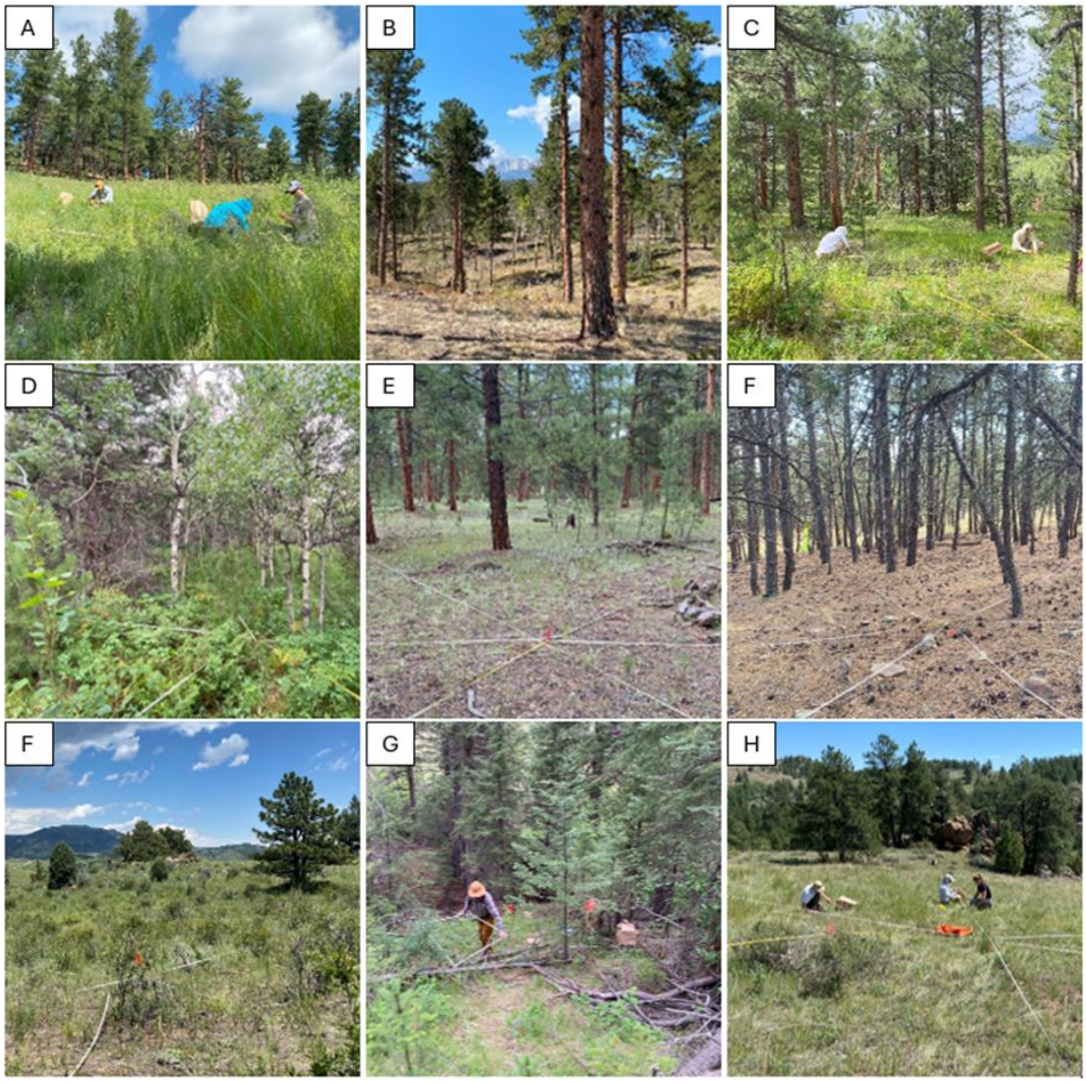

Figure 1.3. Photos of site conditions. (A) Bald Mountain Scenic Area (B) Pikes Peak Forest Dynamics Plot (C&D) Bunce School Road – photos from different plots demonstrating within site variation of conditions (E) Manitou Experimental Forest (F) Centennial Cone Park (G&H) Ben Delatour Scout Ranch, photos from different plots demonstrating within site variation of conditions.

From the center point of each subplot, six 11.4 m long planar intercept transects were installed along azimuths of 0, 60, 120, 180, 240, and 300 (Figure 1.4). Dead, downed, and woody debris were measured along designated sections of each transect: 1-hour (diameter 0-0.6 cm) and 10-hour (diameter 0.6-2.5 cm) fuels were measured along a 1.8 m section of each transect (4.3-6.1 m),

while 100-hour fuels (diameter 2.5-7.6) were measured along a 3.0 m section (4.3-7.3 m). Coarse woody debris (CWD), or 1000-hour fuels (diameter > 7.6 cm), were measured along the full 11.4 m length of each transect. The diameter and decay class of all CWD was recorded according to FIA protocols (USFS, 2018; Tinkham et al., 2018). Decay classes 1 and 2 were combined to indicate sound CWD and decay classes 3-5 were used to indicate rotten CWD for calculation of surface fuel loads according to Brown (1974). At 1.8 m from subplot center on each transect, duff and litter depth were recorded and averaged together to estimate a mean plot level depth. Then 73 canopy cover points were collected every 0.9 m along the transects and at plot center using a GRS densitometer.

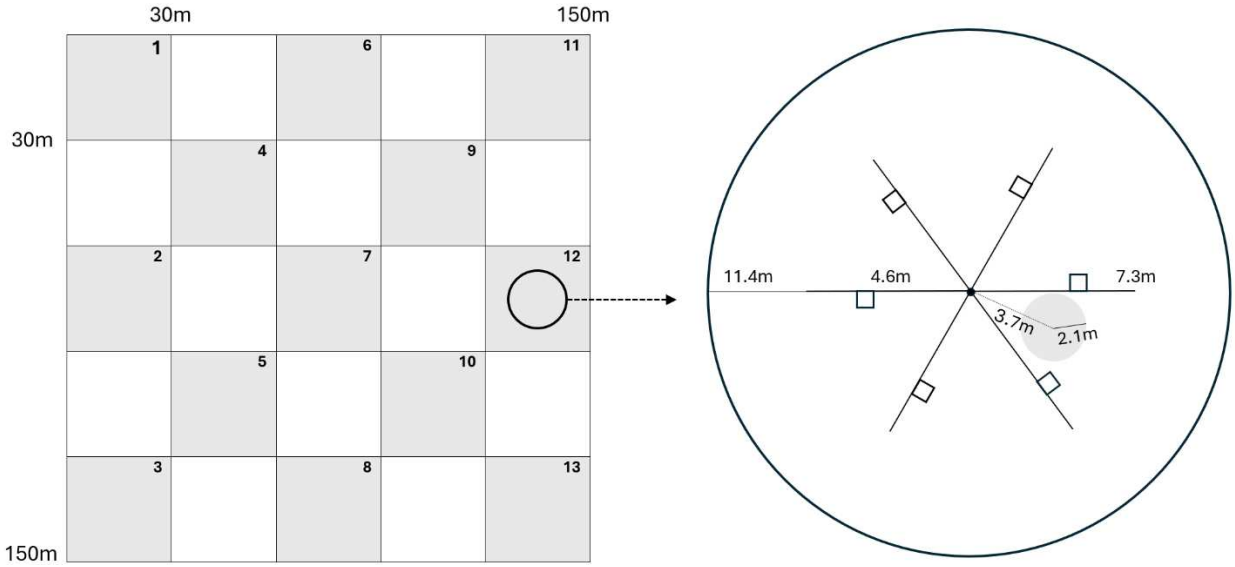

Figure 1.4. Site and plot sampling layout – plots established in alternating shaded and numbered pixels. Surface and ground fuels, and canopy cover measured along each of the six planar transects. Herbaceous and woody fuels were destructively sampled on a 1 m2 quadrat along the left side (from the plot center) of each transect. Trees with a DBH greater than 12.7 cm measured within the 404 m^2 plot, and seedlings and saplings measured in the circular shaded 13 m^2 plot.

Herbaceous and live woody cover and biomass were quantified on six 1 m^2 quadrats located adjacent to each transect 4.6 m from plot center (Figure 1.4). Within each 1 m^2 quadrat, surface cover of bare ground, rock, litter, moss/lichen, live herbaceous vegetation, live woody vegetation, and cacti were ocularly estimated following Daubenmire (1959). All rooted herbaceous vegetation,

woody vegetation, and cacti were collected and transported back to the lab for processing to estimate fuel load. Herbaceous vegetation, woody vegetation, and cacti samples were dried in an oven for 1-3 weeks at 55°C to calculate dry biomass for fuel loading.

2.3. Plot fuel metrics

Fine and coarse dead woody debris loading was calculated at each plot following procedures outlined in Brown (1974). Litter loading was estimated by multiplying the average litter depth per plot by a Colorado Front Range-specific litter bulk density value for ponderosa pine forests of 20.88 kg m^{-3} (Ziegler, 2014). To allow for comparisons across fuel maps, litter, and 1-hour fuels were combined and reported as fine fuels. Live herbaceous and woody vegetation fuel loads were estimated as the means of the 1 m^2 clip plots.

To remain consistent with the methodology employed by LANDFIRE and FastFuels, only live trees with a DBH greater than 12.7 cm were included in the calculation of canopy fuel layer metrics. Canopy top height (TopHt), quadratic mean diameter (QMD), basal area (BA), and trees per hectare (TPha) were estimated following standard forest protocols (Burkhart et al., 2019). The Fire and Fuels Extension (FFE) to the Forest Vegetation Simulator (FVS) (Dixon, 2002; Reinhardt, 2003) was employed to calculate CBH and CBD. FFE-FVS calculates CBD and CBH from a tree list consisting of each tree's species, DBH, height, and crown ratio, along with an expansion factor for plot size. It employs species-specific allometric equations to estimate the biomass of tree components (e.g., foliage and branches) and the crown volume, which is the height of the tree times crown ratio and a shape factor (typically conical for ponderosa pine) and then divides the total crown biomass by the crown volume. Estimated CBD from FFE-FVS is calculated as the maximum 4 m running mean bulk density of predefined 0.3 m thick canopy layers. CBH is estimated as the lowest height at which the running mean bulk density of canopy layer exceeds a predefined threshold of 0.011 kg m^{-3}. The equations used in FVS are consistent with those employed by LANDFIRE.

2.4. LANDFIRE, FCCS, and FastFuels fuel metrics

LANDFIRE's FCCS fuelbeds (LANDFIRE 2.2.0, 2020), Scott and Burgan's (2005) Fire Behavior Fuel Models (FBFM40, LANDFIRE 2.4.0, 2023d), and LANDFIRE canopy metrics (LANDFIRE 2.4.0, 2023a-c) were downloaded from the LANDFIRE website (LANDFIRE, 2024) on 03/07/2024. Subplot center points were recorded in the field using an Emlid Reach RS2+ real-time kinematic (RTK) GPS with a horizontal accuracy of < 0.2 m for each plot and were uploaded as a map layer in QGIS (version 3.38; QGIS, 2023). The LANDFIRE data layers were intersected with the subplot locations in QGIS to identify the collocated field plot with LANDFIRE's FCCS, FBFM40, and canopy fuel metrics.

To estimate FastFuels canopy metrics, 0.09 ha square polygons situated around the plot center of each sampled subplot were imported into the FastFuels SDK dataset in Python (fastfuelsSDK, 2024) and a tree list with the location, DBH, height, canopy base height, crown width, and species was downloaded for each 0.09 ha polygon. CBH and CBD were estimated using the FastFuels tree list and protocols of FFE-FVS (Dixon, 2002; Reinhardt, 2003). Other overstory forest metrics, including QMD, BA, TopHT, and TPha were calculated using standard forestry protocols. FastFuels canopy cover was determined using tree location and canopy width data in ArcGIS Pro (ESRI, 2023) by dissolving the canopy buffers created from the canopy radii and calculating the proportion of each 0.09 ha subplot occupied by canopy. FastFuels surface fuel loads are derived directly from LANDFIRE's FBFM40 fuel load estimates and therefore were not assessed separately in this study.

2.5. Analysis

To assess the performance of LANDFIRE, FCCS, and FastFuels fuel maps, observed versus predicted fuel metrics including mean error (ME), correlation coefficient (R), mean absolute percent error (MAPE), and root mean squared error (RMSE) were calculated for each fuel component. These values were aggregated using site as the experimental variable, thus the 13

subplot values at each site were averaged for a sample size of seven. ME and RMSE represent the direction and magnitude of bias and precision, respectively. MAPE and R provide measures of error and correlation strength in standardized units, allowing comparisons across fuel components with different units and fuel load ranges. Summary statistics were produced using the RStudio integrated development environment (R Core Team, 2022).

To evaluate drivers of error for the fuel components and metrics mapped by LANDFIRE's FBFM40 and FCCS surface fuels and LANDFIRE and FastFuels canopy metrics, linear mixed effects models were fit using ecologically relevant observed predictor variables and assigning site as a random effect. Surface fuel predictors included the observed value of the relative response variable ME (i.e., the predictor variable for FCCS fine fuel load ME would be observed fine fuel load), elevation, slope, cosine transformed aspect, canopy cover, and tree density (ha). Canopy error predictors included all the previous variables with the addition of canopy top height. Variables were reduced using a forward/backward stepwise process to minimize the Akaike Information Criterion. Each of the reduced regression models was checked for variance inflation; resulting multicollinearity for fixed effects ranged from 0 – 3.76, resulting in no further variable removal.

To assess changes in accuracy and bias of individual fuel components and predictor metrics across scales, summary statistics were estimated across 30 m x 30 m (0.09 ha), 60 m x 60 m (0.12 ha), 90 m x 90 m (0.81 ha), 120 m x 120 m (1.44 ha), and 150 m x 150 m (2.25 ha) scales (Figure 1.5). Estimates of each metric from the observed data were calculated by averaging all subplots within a given area. Estimates from LANDFIRE, FCCS, and FastFuels were calculated by averaging data from all pixels within a given scale. Generalized linear models using map spatial scale as the predictor variable and ME as the response variable were constructed in RStudio (R Core Team, 2023) to further evaluate the relationship between map scale and map bias, using a significance level of $\alpha = 0.05$ and site as a random effect.

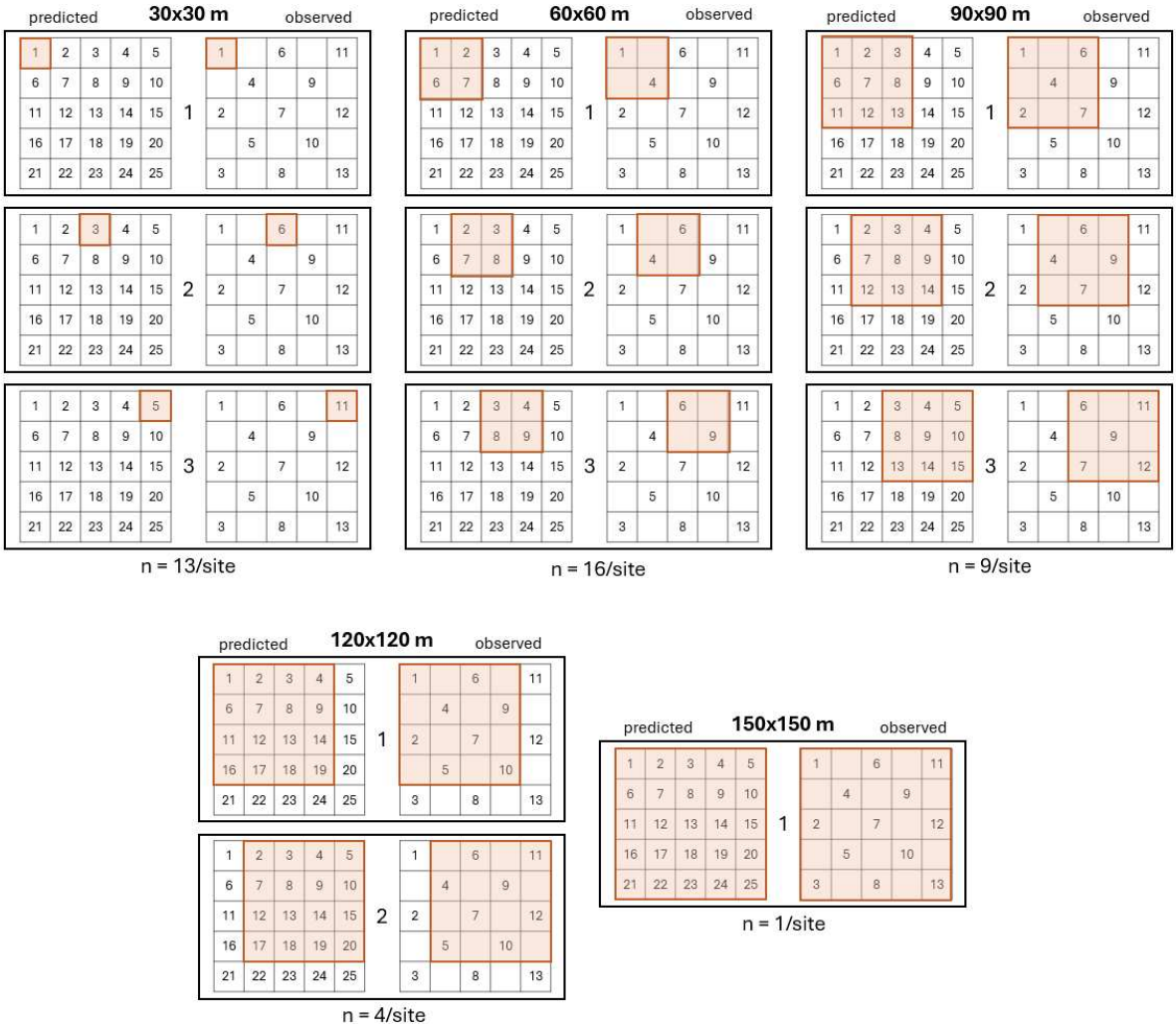

Figure 1.5. Example groupings of predicted and observed pixel comparisons for scaling analysis. Pixel numbers indicate subplot numbers and central numbers between each 5x5 grid indicate the comparison identifier for each scale. The number of comparisons for each scale is indicated below, per site.

3. RESULTS

3.1. Site summaries

Measured stand density, tree size, and surface and canopy fuel metrics varied both within and between sites (Table 1.2). Among surface fuel components, average fine fuel loads (litter and 1-hour fuels) ranged from 0.21 to 0.53 kg m^{-2}, while coarse fuel loads (1000-hour fuels) ranged from 0.22 to 1.39 kg m^{-2} across sites. Herbaceous and shrub fuel load averages ranged between 0.01-0.08 kg m^{-2} and 0.01-0.22 kg m^{-2}, respectively. Within sites, relative standard deviations (RSDs)

ranged between 21-78% for fine fuels, 70-193% for coarse fuels, 30-184% for herbaceous fuels, and 73-334% for shrub fuels.

Across all subplots (n = 91), LANDFIRE assigned seven FBFM40 surface fuel models, with four fuel models representing 90% of the subplots. Ten FCCS fuelbeds were assigned to the 91 subplots with one fuelbed representing 75% of all subplots, and 90% being represented by three fuelbeds. Three sites, including Bald Mountain Scenic Area, Heil Valley Ranch, and the Manitou Experimental Forest were each designated entirely by FCCS fuelbed 228 – "Interior ponderosa pine – limber pine forest". No sites were described by less than two FBFM40 fuel models.

Mean tree density ranged from 127 to 971 trees ha^{-1} across sites, exhibiting the greatest within-site variation of the canopy metrics with RSDs ranging from 30-106% (Table 1.2). Average QMD ranged from 20-39 cm between sites and had the least within-site variation ranging from 11-37% RSD. The variation in tree size and stand density propagated through to represent mean site CBHs of 1.4-4.8 m, while within site RSD of CBH ranged from 31-78%.

Table 1.2. Measured site attributes, means, and standard deviations (in parentheses). Total surface fuel load includes the average litter, 1-, 10-, 100- and 1000-hour down and dead woody debris, and live herbaceous and shrub loads. Tree density and quadratic mean diameter (QMD) only include trees over 12.7 cm diameter. BA: basal area; CBH: canopy base height.

Site	Tree Density (ha)	QMD (cm)	BA (m^2 ha^{-1})	Canopy Height (m)	CBH (m)	Total Surface Fuel Load (kg m^{-2})
Ben Delatour Scout Ranch	213 (159)	29.1 (6.8)	12.5 (8.9)	10.9 (6.1)	2.1 (1.1)	2.24 (2.95)
Heil-Valley Ranch	971 (296)	20.1 (4.4)	30.5 (16.8)	8.9 (2.1)	2.1 (0.8)	1.14 (0.24)
Bunce School Road (Wallace)	559 (254)	26.0 (4.8)	28.9 (11.8)	12.4 (2.6)	1.4 (1.1)	1.87 (1.05)
Bald Mountain Scenic Area	179 (103)	38.5 (7.9)	18.0 (5.5)	14.4 (2.0)	2.4 (1.0)	1.57 (1.25)
Centennial Cone Park	127 (135)	32.3 (11.9)	7.9 (6.2)	8.9 (2.1)	1.8 (1.1)	0.79 (0.53)
Manitou Experimental Forest (N1)	295 (110)	33.5 (3.6)	26.0 (10.3)	19.2 (2.2)	4.8 (1.5)	1.42 (1.10)
Pikes Peak Forest Dynamics Plot	163 (82)	32.4 (10.3)	12.0 (5.2)	14.9 (2.9)	3.6 (2.8)	2.85 (1.84)

3.2. Fine-scale evaluation

3.2.1. Surface fuels

The agreement between observed fuel loading and FCCS estimates of surface fuel components were highly variable at the finest scale of analysis (0.09 ha). Fine fuel loads were the most accurately predicted component, with a ME of 0.12 kg m^{-2} and MAPE of 36% (Table 1.3). Errors among other dead, down, and woody fuels ranged between 53% and 143% MAPE, with the greatest error associated with coarse woody (1000-hour) fuels which had a ME of -0.62 kg m^{-2}. Shrub fuel loads were the least accurately estimated FCCS component with a ME of -0.46 kg m^{-2}, translating to a MAPE of 2590%. FCCS consistently underpredicted fine, 10-hour, and 100-hour fuels while overpredicting coarse woody fuels, herbaceous, and shrub fuel loads (Figure 1.6).

FCCS estimates of 10-hour, 100-hour, 1000-hour, and herbaceous fuels showed varying degrees of positive correlation with observed fuel loadings (Table 1.3). Correlation coefficients ranged from 0.12 for herbaceous fuels up to 0.85 for 100-hour fuels. Notably, FCCS estimates of fine and shrub fuel loads exhibited moderate and strong negative correlations with observed values, indicating that as observed fuel loads increased, FCCS estimates decreased.

Table 1.3. FCCS observed – predicted (kg m^{-2}) surface fuel summary statistics including mean observed fuel load and (standard deviation), mean predicted FCCS fuel load and (standard deviation), mean error (ME), correlation coefficient (R), mean absolute percent error (MAPE), and root mean squared error (RMSE).

Fuel Component	Mean Observed	Mean Predicted	ME	R	MAPE	RMSE
Fine fuels (kg m^{-2})	0.37 (0.13)	0.26 (0.03)	0.12	-0.51	36	0.18
10-hour (kg m^{-2})	0.23 (0.1)	0.17 (0.03)	0.07	0.24	53	0.11
100-hour (kg m^{-2})	0.42 (0.41)	0.23 (0.12)	0.19	0.85	103	0.35
1000-hour (kg m^{-2})	0.67 (0.42)	1.28 (0.71)	-0.62	0.26	143	0.93
Herbaceous (kg m^{-2})	0.05 (0.03)	0.06 (0.02)	-0.01	0.12	137	0.03
Shrub (kg m^{-2})	0.1 (0.08)	0.55 (0.16)	-0.46	-0.91	2590	0.51

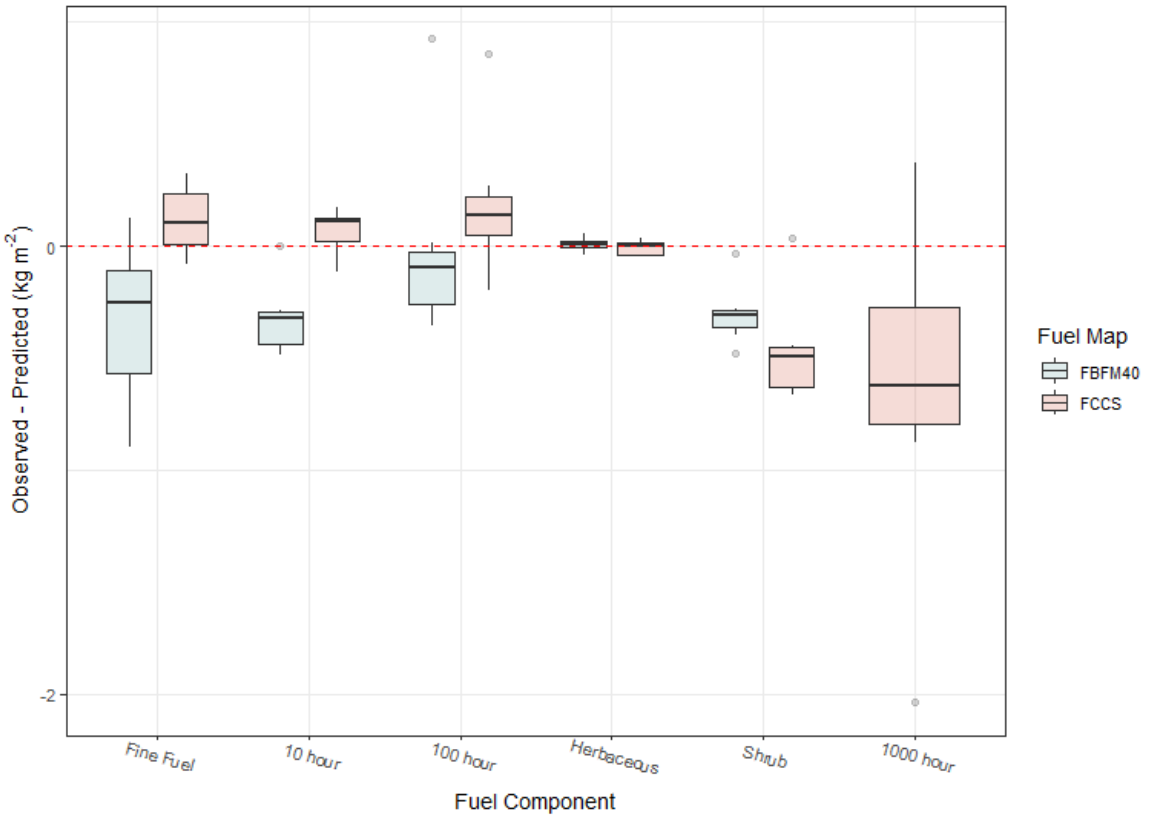

Figure 1.6. Distribution of observed – predicted LANDFIRE 40 Scott and Burgan Fire Behavior Fuel Models (FBFM40) and Fuel Characteristic Classification fuelbeds (FCCS) surface fuel loads. Boxes represent the interquartile range of the observed – predicted surface fuel loads, tails extend to capture the 95% confidence interval, and outliers are represented by circles beyond the 95% confidence interval.

Mean errors of LANDFIRE FBFM40 surface fuel component estimates were also highly variable but exhibited a narrower range and higher median error for the surface fuel layer compared to FCCS estimates (Table 1.4). Among FBFM40 components, herbaceous fuels were the most accurately estimated, with a ME of 0.01 kg m^{-2} and a corresponding MAPE of 61%. Mean absolute percent errors for fine, 10-hour, and 100-hour fuels ranged from 103% to 204%. While the FBFM40 shrub loads were improved compared to the FCCS estimates, they were still the least accurately estimated fuel component with a ME of -0.3 and MAPE of 1630%. FBFM40 surface fuel load estimates were overpredicted relative to field-derived estimates for all surface fuel components except herbaceous fuel loads (Figure 1.6).

Table 1.4. LANDFIRE FBFM40 observed – predicted (kg m^{-2}) surface fuel summary statistics including mean observed fuel load and (standard deviation), mean predicted FBFM40 fuel load and (standard deviation), mean error (ME), correlation coefficient (R), mean absolute percent error (MAPE), and root mean squared error (RMSE).

Fuel Component	Mean Observed	Mean Predicted	ME	R	MAPE	RMSE
Fine fuels (kg m^{-2})	0.37 (0.13)	0.70 (0.41)	-0.33	0.57	103	0.46
10-hour (kg m^{-2})	0.23 (0.1)	0.55 (0.12)	-0.31	-0.02	204	0.35
100-hour (kg m^{-2})	0.42 (0.41)	0.43 (0.08)	-0.01	-0.05	166	0.39
Herbaceous (kg m^{-2})	0.05 (0.03)	0.04 (0.04)	0.01	0.73	61	0.03
Shrub (kg m^{-2})	0.1 (0.08)	0.39 (0.06)	-0.3	-0.76	1630	0.32

FBFM40 estimates of fine and herbaceous fuel loads positively correlated observed fuel loads, exhibiting moderate to strong relationships (R=0.57 and R=0.73, respectively). The remaining surface fuel components exhibited negative correlations with observed fuel loads ranging from very weak negative relationships for 10- and 100-hour fuels (R = -0.02 and R=-0.05) to a strong negative correlation of shrub fuel load estimates (R=-0.91).

3.2.2. Canopy fuels

Errors derived from LANDFIRE-based estimates of the canopy fuel complex were the least variable and had the lowest range of MAPE values (24-54%) among the evaluated fuel maps (Table 1.5). CBH was the least accurately estimated metric, with a ME of 1.44 m and MAPE of 54%. Despite CBD being unbiased, the limited variation in predictions led to a MAPE of 42%. Canopy top height was the most accurately estimated metric, with a ME of 1.11 m and MAPE of 24%. All canopy metrics derived from LANDFIRE were underpredicted compared to field-based estimates, except canopy top height, which was overpredicted.

Correlations between LANDFIRE-derived and field-derived estimates were all positive but varied in strength. CBH showed a weak correlation (R=0.13), while canopy top height had a moderate correlation (R=0.53), and CBD exhibited a strong correlation (R=0.75). Estimated canopy cover was LANDFIRE's most strongly correlated variable with field-derived estimates (R=0.91).

Table 1.5. LANDFIRE observed – predicted canopy summary statistics including mean observed canopy metrics and (standard deviation), mean predicted LANDFIRE canopy metrics and (standard deviation), mean error (ME), correlation coefficient (R), mean absolute percent error (MAPE), and root mean squared error (RMSE). CBD: canopy bulk density; CBH: canopy base height; TopHt: canopy top height; CC: canopy cover.

Fuel Component	Mean Observed	Mean Predicted	ME	R	MAPE	RMSE
CBD (kg m^{-3})	0.08 (0.06)	0.08 (0.02)	0.01	0.75	42	0.05
CBH (m)	2.54 (1.24)	1.10 (0.92)	1.44	0.13	54	1.97
TopHt (m)	12.8 (3.70)	13.9 (3.17)	-1.11	0.53	24	3.31
CC (%)	47.0 (24.5)	39.6 (10.3)	7.38	0.91	30	16.3

The accuracy of canopy metrics derived from FastFuels data was more variable than those derived from LANDFIRE data. MAPE of FastFuels canopy metrics ranged from a low of 22% for canopy to height to a high of 136% for CBH (Table 1.6). Estimates of top height, CC, and CBH were overpredicted on average by 3.67 m, 5.5%, and 2.25 m respectively, while CBD was underpredicted by 0.05 kg m^{-3} (Figure 1.7). Because FastFuels relies on a tree list, additional metrics of forest canopy beyond CC, CBH, CBD, and top height can be evaluated. Trees per hectare, QMD, and BA were all overpredicted with MAPEs ranging from 23-43%.

Correlations between FastFuels derived metrics and field derived metrics varied in strength and direction. CBD and CBH exhibited moderate inverse correlations (R=-0.45 and R=-0.32), indicating that as fuel load increases FastFuels estimates tend to decrease. However, canopy cover (R=0.14), top height (R=0.26), trees per hectare (R=0.36), basal area (R=0.42), and QMD (R=0.42) were positively correlated with observed values.

Table 1.6. FastFuels observed – predicted canopy summary statistics of mean observed canopy metric and (standard deviation), mean FastFuels' predicted canopy metric and (standard deviation), mean error (ME), correlation coefficient (R), mean absolute percent error (MAPE), and root mean squared error (RMSE). Metrics from trees > 12.7 cm diameter at breast height (DBH). CBD: canopy bulk density; CBH: canopy base height; TopHt: canopy top height; CC: canopy cover; QMD: quadratic mean diameter; BA: basal area.

Fuel Component	Mean Observed	Mean Predicted	ME	R	MAPE	RMSE
CBD (kg m^{-3})	0.08 (0.06)	0.03 (0.01)	0.05	-0.45	52	0.08
CBH (m)	2.54 (1.24)	4.79 (1.64)	-2.25	-0.32	136	3.13
TopHt (m)	12.8 (3.70)	13.2 (2.25)	-3.67	0.26	22	3.54
CC (%)	47.0 (24.5)	52.5 (28.7)	-5.49	0.14	79	32.8
Trees ha^{-1}	145 (124)	92.9 (27.8)	52.1	0.36	34	120
QMD (cm)	29.5 (6.0)	24.4 (2.9)	5.10	0.42	23	7.17
BA (m^2 ha^{-1})	19.6 (9.0)	10.8 (3.4)	8.74	0.42	43	11.5

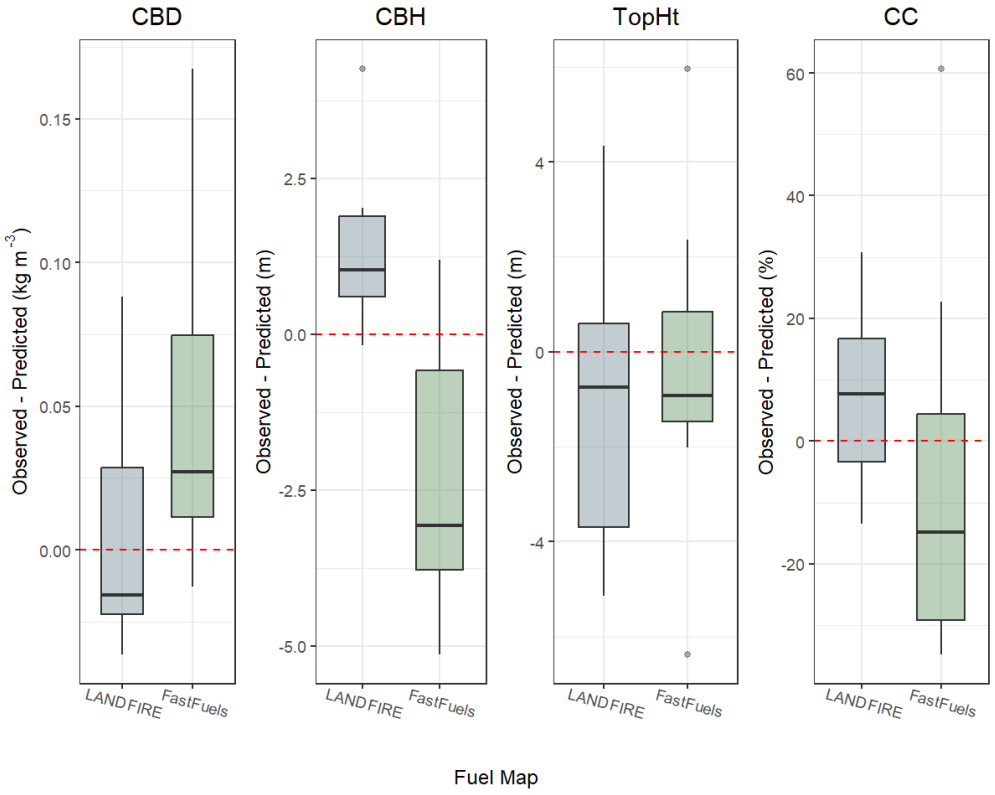

Figure 1.7. Distribution of observed – predicted LANDFIRE and FastFuel canopy metrics of canopy bulk density (CBD), canopy base height (CBH), canopy top height (TopHt), and canopy cover (CC). Boxes represent the interquartile range, the average value is the black line, tails extend to the 95% confidence interval, and outliers are represented by circles beyond the 95% confidence interval.

3.3. Fine-scale average error regression analysis.

Mean errors of surface fuel metrics varied between products and were influenced by forest structure and topography, with differences in the relationships occurring among fuel components. Mean errors for all FBFM40 and FCCS surface fuel components were positively correlated with observed values (Table 1.7). For FBFM40 components, no significant predictors related error to forest structure or topography, except for fine fuel error, which showed a slight negative relationship with tree density.

Relationships between mean errors of FCCS surface fuel components and topographic and forest structure variables were weak (≤0.01; Table 1.7). FCCS fine and 10-hour fuel load errors were inversely correlated with slope and elevation but showed no clear relationship with forest structure. Errors for larger-diameter dead down and woody fuels, as well as shrub fuels, were more strongly associated with forest structure metrics. Specifically, errors in 100- and 1000-hour fuel loads were inversely related to canopy cover and positively correlated with tree density, while shrub fuel load error showed the opposite pattern, being positively correlated with canopy cover and inversely related to tree density. Herbaceous fuel load error was not influenced by any additional predictors (Table 1.7).

Mean errors of LANDFIRE and FastFuels canopy metrics were also weakly influenced (≤0.01) by forest structure and topographic variables, with relationships varying among fuel maps and canopy metrics (Table 1.7). Again, mean errors of all LANDFIRE and FastFuels canopy metrics were positively correlated with observed values. LANDFIRE metrics displayed inverse correlations with forest structure and topographic variables, such as CBH negatively related to elevation, CBD negatively related to tree density, and canopy top height negatively related to both elevation and tree density. For FastFuels metrics, fewer predictors were significant, with CBH error positively correlated to elevation and CBD error inversely correlated to canopy top height.

Table 1.7. Linear mixed effects models of fuel metric errors from observed – predicted 40 Fire Behavior Fuel Models (FBFM40), Fuel Characteristic Classification System (FCCS), LANDFIRE (LF), and FastFuels (FF) fuel maps against fixed effects of observed value, slope, elevation, aspect (cosine transformation), canopy cover (CC), trees per hectare (TPha) ≥12.7 cm DBH, and canopy top height (TopHt), using site as a random effect. Under model strength, the first number is marginal R^2, or the proportion of variance explained by the fixed effects (predictor variables), and the second number is the conditional R^2, or variance explained by fixed and random effects. Only significant relationships are included, blanks indicate non-significant relationships. Estimates indicate the relative unit increase in mean error per unit increase in the relative predictor variable.

Fuel Map	Response Variable Error	Model Strength	Predictor Variables						
			Observed Variable Estimate	Slope (%)	Elevation (m)	Aspect	CC (%)	TPha	TopHt (m)
FBFM40	Fine fuels	0.198/0.529	1.2503					-0.0005	
FBFM40	10 hr	0.092/0.145	0.6480						
FBFM40	100 hr	0.866/NA	0.9764						
FBFM40	Herbaceous	0.305/0.455	0.9115						
FBFM40	Shrub	0.323/NA	1.0493						
FCCS	Fine fuels	0.884/0.899	0.9358	-0.0013					
FCCS	10 hr	0.889/NA	0.9394	-0.0015	-0.0001				
FCCS	100 hr	0.921/0.974	0.9941				-0.0044	0.0002	
FCCS	1000 hr	0.569/0.864	0.9235				-0.0127	0.0008	
FCCS	Herbaceous	0.393/0.413	0.9334						
FCCS	Shrub	0.406/0.822	1.0537				0.0054	-0.0002	
LF	CBH	0.501/NA	1.1874		-0.0034				
LF	CBD	0.823/0.850	1.0507					-0.0000	
LF	CC	0.811/0.859	0.7610				---		
LF	TopHt	0.612/0.692	0.6748		-0.0077			-0.0066	---
FF	CBH	0.437/0.502	1.0614		0.0053				
FF	CBD	0.328/0.709	0.9957						-0.0017
FF	CC	0.328/0.709	0.9772				---		
FF	TopHt	0.513/0.667	0.9038						---

3.4. Fuel map accuracies across increasing scales

Regardless of fuel component or mapping product, there were no significant relationships (α = 0.05) between mean errors of surface fuel load and scale (Figure 1.8, Figure 1.9). FCCS fuel maps underpredict fine, 10- and 100-hour fuel loading across all scales, and overpredict 1000-hour, herbaceous, and shrub fuel loads across map scales (Figure1. 8, Table 1.8). FBFM40 surface fuel estimates were greater than measured values for all fuel components and scales except

herbaceous fuel loads which maintained underpredictions across scales (Figure1. 8, Table 1.9). MAPE and correlation strength (R) of FCCS and FBFM40 surface fuel components show no other significant or consistent trends across scales.

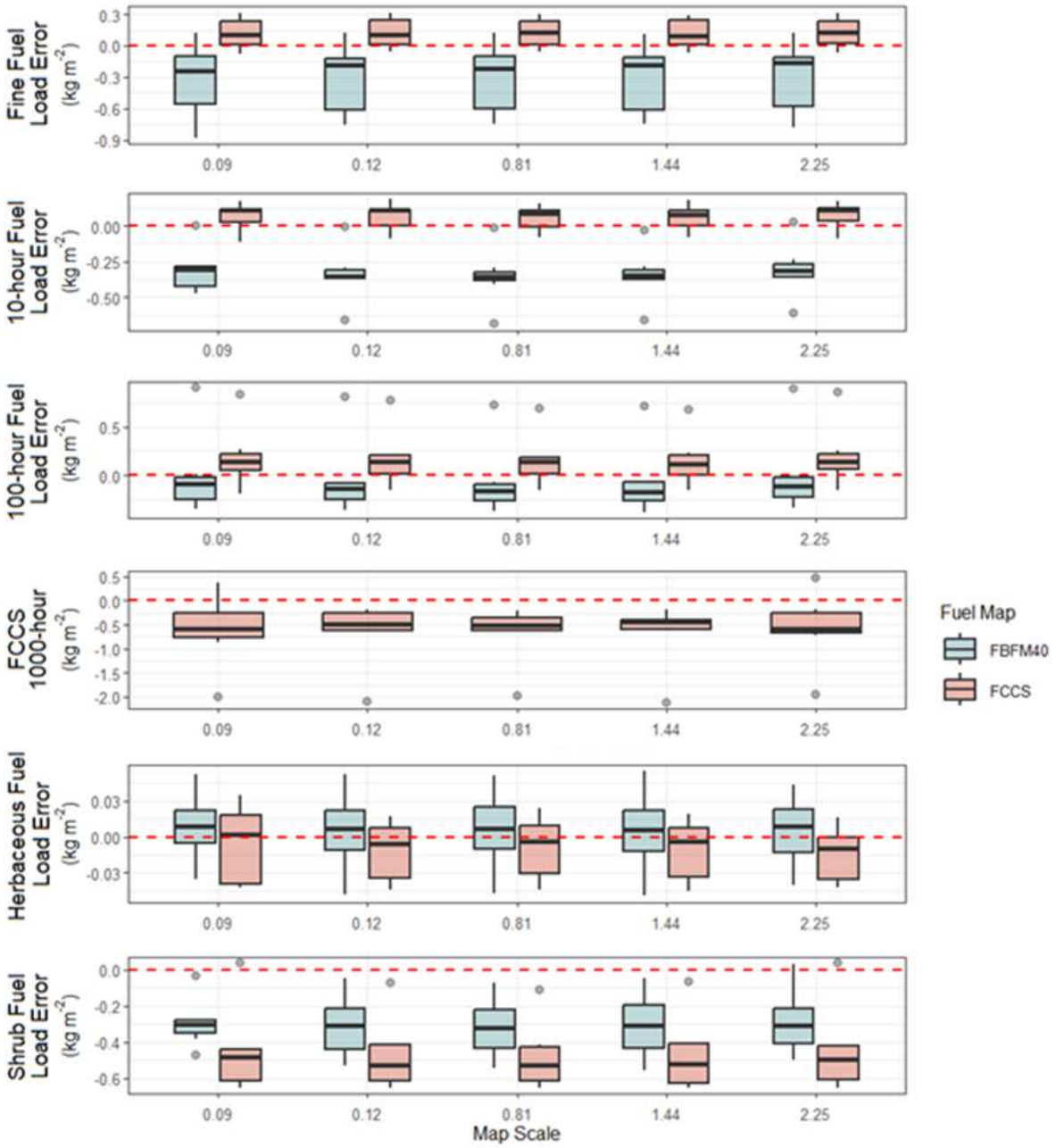

Figure 1.8. Boxplot of surface fuel component observed – predicted FBFM40 and FCCS loads across increasing scales from 0.09-2.25 ha. Boxes represent the interquartile range, tails extend to capture the 95% confidence interval, and circles are outliers beyond the 95% confidence interval.

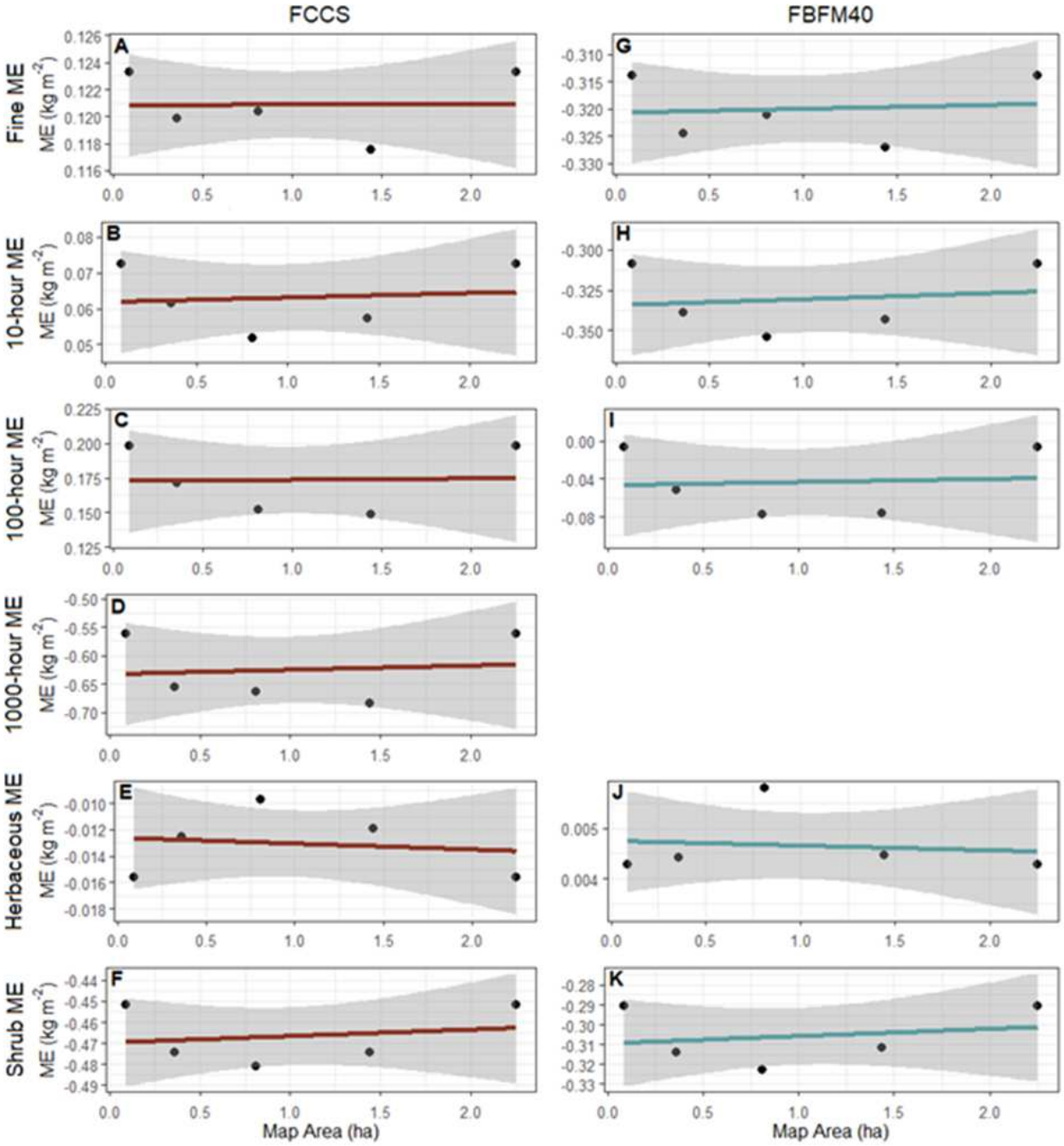

Figure 1.9. Generalized linear model (GLM) of FBFM40 and FCCS surface fuel component mean errors (ME) across increasing map resolutions. Panels A-F show GLM of FCCS ME surface fuel estimates and panels G-K show FBFM40 ME surface fuel estimates.

Table 1.8. FCCS observed - predicted surface fuel load (kg m^{-2}) summary statistics across increasing map scales from 0.09-2.25 ha. Summary statistics include mean observed fuel load and (standard deviation), mean predicted FCCS fuel load and (standard deviation), mean error (ME), correlation coefficient (R), mean absolute percent error (MAPE), and root mean squared error (RMSE).

Map Scale	Fuel Component	Mean Observed	Mean Predicted	ME	R	MAPE	RMSE
0.09 (ha)	Fine fuels (kg m^{-2})	0.37 (0.13)	0.26 (0.03)	0.12	-0.51	36	0.18
	10-hour (kg m^{-2})	0.23 (0.1)	0.17 (0.03)	0.07	0.24	53	0.11
	100-hour (kg m^{-2})	0.42 (0.41)	0.23 (0.12)	0.19	0.85	103	0.35
	1000-hour (kg m^{-2})	0.67 (0.42)	1.28 (0.71)	-0.62	0.26	143	0.93
	Herbaceous (kg m^{-2})	0.05 (0.03)	0.06 (0.02)	-0.01	0.12	137	0.03
	Shrub (kg m^{-2})	0.1 (0.08)	0.55 (0.16)	-0.46	-0.91	2590	0.51
0.36 (ha)	Fine fuels (kg m^{-2})	0.37 (0.14)	0.25 (0.01)	0.12	-0.31	35	0.18
	10-hour (kg m^{-2})	0.22 (0.1)	0.16 (0.02)	0.06	0.26	53	0.11
	100-hour (kg m^{-2})	0.38 (0.38)	0.21 (0.10)	0.17	0.87	140	0.33
	1000-hour (kg m^{-2})	0.55 (0.22)	1.20 (0.71)	-0.66	0.37	141	0.9
	Herbaceous (kg m^{-2})	0.05 (0.03)	0.06 (0.02)	-0.01	0.68	157	0.03
	Shrub (kg m^{-2})	0.09 (0.07)	0.56 (0.14)	-0.47	-0.75	2884	0.51
0.81 (ha)	Fine fuels (kg m^{-2})	0.37 (0.14)	0.24 (0.01)	0.12	-0.35	36	0.18
	10-hour (kg m^{-2})	0.21 (0.09)	0.16 (0.02)	0.05	0.24	49	0.1
	100-hour (kg m^{-2})	0.36 (0.35)	0.21 (0.10)	0.15	0.89	137	0.29
	1000-hour (kg m^{-2})	0.53 (0.23)	1.2 (0.71)	-0.66	0.6	142	0.87
	Herbaceous (kg m^{-2})	0.05 (0.02)	0.06 (0.02)	-0.01	0.63	147	0.03
	Shrub (kg m^{-2})	0.09 (0.07)	0.57 (0.14)	-0.48	-0.57	2996	0.51
1.44 (ha)	Fine fuels (kg m^{-2})	0.36 (0.14)	0.25 (0.01)	0.12	-0.33	36	0.18
	10-hour (kg m^{-2})	0.21 (0.09)	0.16 (0.02)	0.06	0.20	49	0.10
	100-hour (kg m^{-2})	0.36 (0.35)	0.10 (0.10)	0.15	0.87	137	0.29
	1000-hour (kg m^{-2})	0.52 (0.18)	1.20 (0.71)	-0.68	0.47	144	0.91
	Herbaceous (kg m^{-2})	0.05 (0.03)	0.06 (0.02)	-0.01	0.67	182	0.03
	Shrub (kg m^{-2})	0.09 (0.08)	0.57 (0.14)	-0.47	-0.69	2896	0.51
2.25 (ha)	Fine fuels (kg m^{-2})	0.37 (0.13)	0.25 (0.03)	0.12	-0.29	35	0.18
	10-hour (kg m^{-2})	0.23 (0.1)	0.16 (0.02)	0.07	0.48	49	0.11
	100-hour (kg m^{-2})	0.42 (0.41)	0.22 (0.11)	0.2	0.89	94	0.36
	1000-hour (kg m^{-2})	0.67 (0.42)	1.23 (0.71)	-0.56	0.24	135	0.88
	Herbaceous (kg m^{-2})	0.05 (0.03)	0.06 (0.02)	-0.02	0.68	125	0.03
	Shrub (kg m^{-2})	0.09 (0.08)	0.54 (0.16)	-0.45	-0.92	2569	0.50

Table 1.9. FBFM40 observed - predicted surface fuel load (kg m^{-2}) summary statistics across increasing map scales from 0.09-2.25 ha. Summary statistics include mean observed fuel load and (standard deviation), mean predicted FCCS fuel load and (standard deviation), mean error (ME), correlation coefficient (R), mean absolute percent error (MAPE), and root mean squared error (RMSE).

Map Scale	Fuel Component	Mean Observed	Mean Predicted	ME	R	MAPE	RMSE
0.09 (ha)	Fine fuels (kg m^{-2})	0.37 (0.13)	0.69 (0.42)	-0.31	0.67	95	0.45
	10-hour (kg m^{-2})	0.23 (0.1)	0.54 (0.18)	-0.31	0.21	183	0.35
	100-hour (kg m^{-2})	0.42 (0.41)	0.42 (0.13)	-0.01	0.15	122	0.38
	Herbaceous (kg m^{-2})	0.05 (0.03)	0.05 (0.05)	0.00	0.76	65	0.03
	Shrub (kg m^{-2})	0.1 (0.08)	0.38 (0.12)	-0.29	-0.63	1513	0.33
0.36 (ha)	Fine fuels (kg m^{-2})	0.37 (0.14)	0.69 (0.42)	-0.32	0.69	100	0.45
	10-hour (kg m^{-2})	0.22 (0.1)	0.56 (0.19)	-0.34	0.3	214	0.38
	100-hour (kg m^{-2})	0.38 (0.38)	0.43 (0.14)	-0.05	0.12	216	0.37
	Herbaceous (kg m^{-2})	0.05 (0.03)	0.05 (0.05)	-0.00	0.71	67	0.03
	Shrub (kg m^{-2})	0.09 (0.07)	0.40 (0.12)	-0.31	-0.55	1700	0.35
0.81 (ha)	Fine fuels (kg m^{-2})	0.37 (0.14)	0.69 (0.41)	-0.32	0.68	100	0.45
	10-hour (kg m^{-2})	0.21 (0.09)	0.56 (0.2)	-0.35	0.24	227	0.4
	100-hour (kg m^{-2})	0.36 (0.35)	0.44 (0.14)	-0.08	0.09	242	0.35
	Herbaceous (kg m^{-2})	0.05 (0.02)	0.05 (0.05)	0.01	0.7	68	0.03
	Shrub (kg m^{-2})	0.09 (0.07)	0.41 (0.12)	-0.32	-0.42	1777	0.36
1.44 (ha)	Fine fuels (kg m^{-2})	0.36 (0.14)	0.69 (0.42)	-0.33	0.69	100	0.45
	10-hour (kg m^{-2})	0.21 (0.09)	0.56 (0.19)	-0.34	0.37	211	0.38
	100-hour (kg m^{-2})	0.36 (0.35)	0.43 (0.14)	-0.08	0.11	232	0.35
	Herbaceous (kg m^{-2})	0.05 (0.03)	0.05 (0.05)	0.00	0.67	69	0.03
	Shrub (kg m^{-2})	0.09 (0.08)	0.40 (0.12)	-0.31	-0.61	1744	0.35
2.25 (ha)	Fine fuels (kg m^{-2})	0.37 (0.13)	0.69 (0.42)	-0.32	0.67	95	0.45
	10-hour (kg m^{-2})	0.23 (0.1)	0.54 (0.18)	-0.31	0.21	183	0.35
	100-hour (kg m^{-2})	0.42 (0.41)	0.42 (0.13)	-0.01	0.15	122	0.38
	Herbaceous (kg m^{-2})	0.05 (0.03)	0.05 (0.05)	0.00	0.76	65	0.03
	Shrub (kg m^{-2})	0.09 (0.08)	0.38 (0.12)	-0.29	-0.63	1513	0.33

Similar to trends in mean error for surface fuel loads, neither LANDFIRE nor FastFuels canopy fuel mean errors showed any statistically significant ($\alpha = 0.05$) relationship to map scale (Figure 1.10, Figure 1.11). However, the mean error of CBD estimates from FastFuels and the top height and canopy cover from LANDFIRE all showed a slight trend ($\alpha = 0.1$) with map scale (Figure 1.11). These trends were not consistent with FastFuels-derived CBD having greater mean error at larger scales and the LANDFIRE-derived CC and top height both having lower mean errors at larger scales (Figure 1.10, Table 1.10). FastFuels canopy metrics continued to underpredict CBD, BA, QMD, and tree density, and overpredict CBH, CC, and canopy top height across increasing scales (Figure 1.10). LANDFIRE estimates of CBD, CBH, and CC maintained overpredictions across all map scales, while canopy top height was underestimated across all scales (Figure 1.10, Table 1.11).

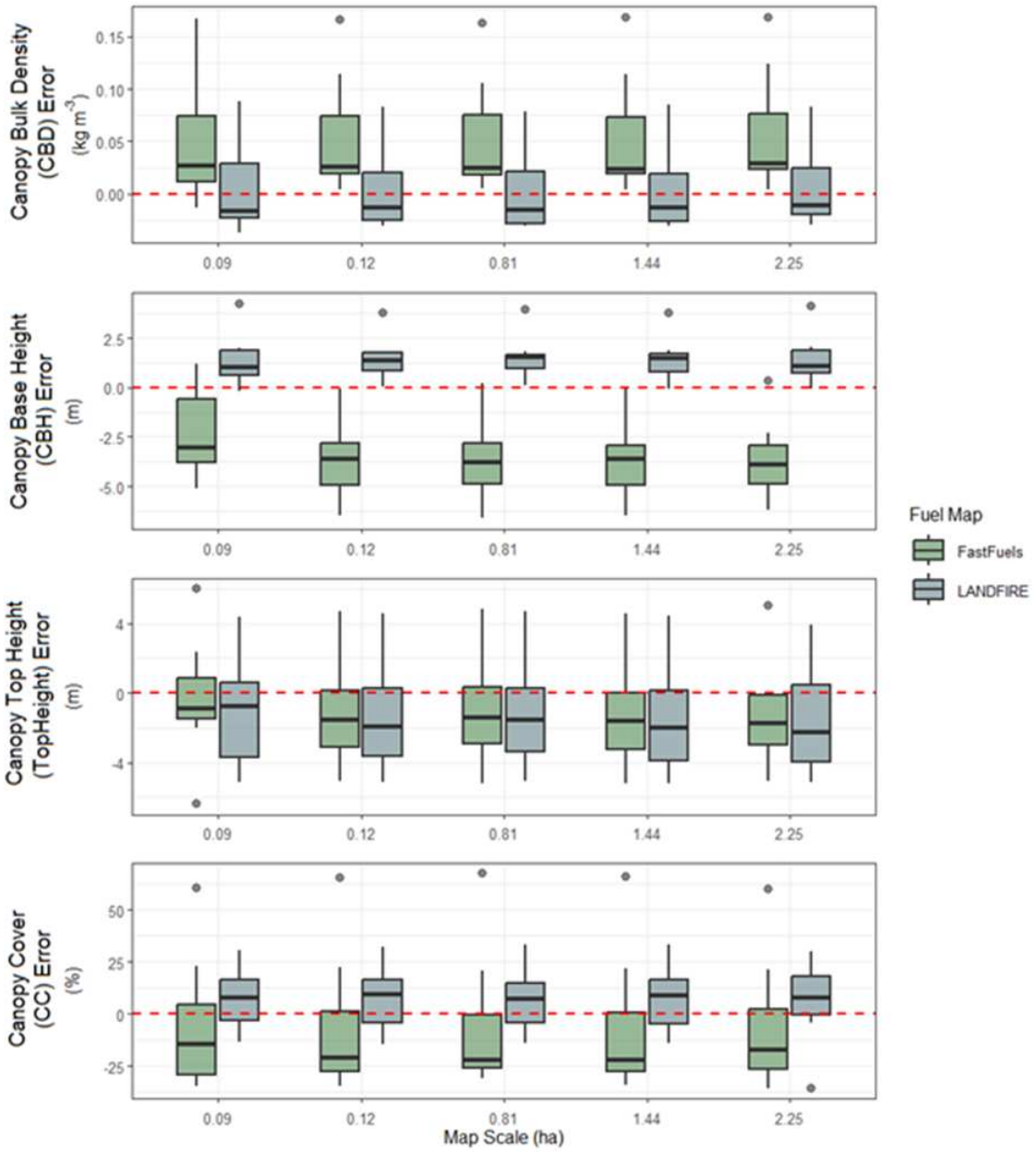

Figure 1.10. Distribution of FastFuels and LANDFIRE canopy metrics across increasing spatial scales. Panels A-G correspond to observed – predicted FastFuels canopy metrics across increasing scales; panels H-K correspond to LANDFIRE observed – predicted canopy metrics across increasing scales.

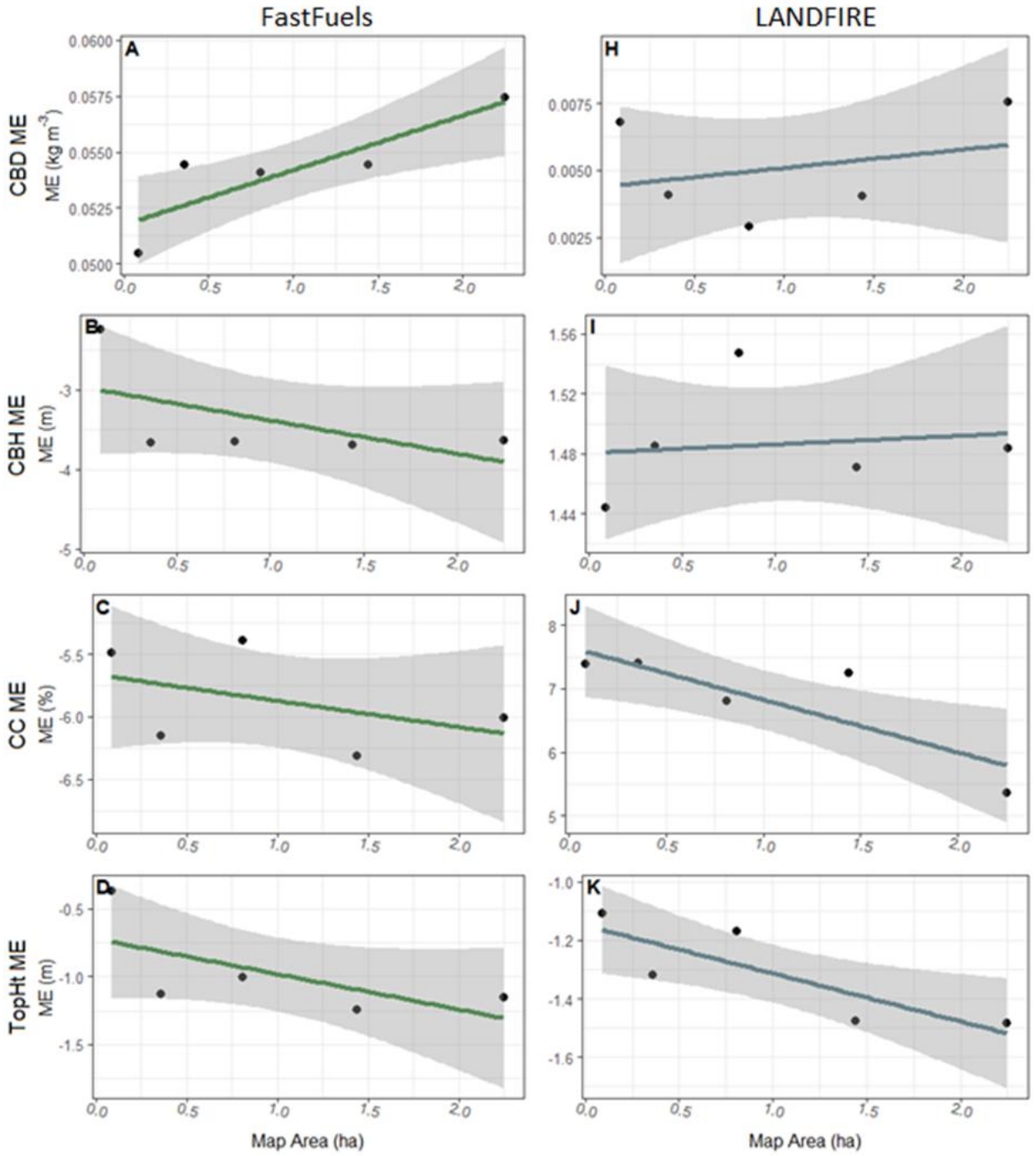

Figure 1.11. Generalized linear models (GLM) of FastFuels and LANDFIRE canopy metric mean errors (ME) across increasing map resolutions. Panels A-D show GLM of FastFuels ME canopy metric estimates and panels I-K show LANDFIRE canopy metric estimates. CBD: canopy bulk density; CBH: canopy base height; CC: canopy cover; TopHt: canopy top height.

Table 1.10. FastFuels observed – predicted canopy metric summary statistics across increasing map scales from 0.09-2.25 ha. Summary statistics include mean observed fuel metric and (standard deviation), mean predicted FastFuels fuel metric and (standard deviation), mean error (ME), correlation coefficient (R), mean absolute percent error (MAPE), and root mean squared error (RMSE). Summary statistics of observed – canopy metrics at increasing map scales. CBD: canopy bulk density; CBH: canopy base height; TopHt: canopy top height; CC: canopy cover; BA: basal area; QMD: quadratic mean diameter.

Map Scale	Canopy Attribute	Mean Observed	Mean Predicted	ME	R	MAPE	RMSE
0.09 (ha)	CBD (kg m^{-3})	0.08 (0.06)	0.03 (0.01)	0.05	-0.45	50	0.08
	CBH (m)	2.54 (1.24)	4.79 (1.64)	-2.25	-0.32	136	3.13
	TopHt (m)	12.82 (3.70)	13.18 (2.25)	-0.37	0.26	22	3.54
	CC (%)	47 (24.45)	52.49 (28.66)	-5.49	0.14	79	32.81
	BA (m^2 ha^{-1})	19.55 (8.97)	10.81 (3.44)	8.74	0.42	43	11.55
	QMD (cm)	29.53(5.99)	24.43 (2.9)	5.10	0.42	23	7.17
	Trees ha^{-1}	145 (124)	93 (28)	52.02	0.36	52	120.23
0.36 (ha)	CBD (kg m^{-3})	0.08 (0.06)	0.02 (0.01)	0.05	0.01	54	0.08
	CBH (m)	2.59 (1.05)	6.26 (1.35)	-3.67	-0.50	178	4.15
	TopHt (m)	12.80 (3.57)	13.93 (1.32)	-1.13	0.46	23	3.16
	CC (%)	45.53 (25.47)	51.68 (29.22)	-6.15	0.11	87	34.45
	BA (m^2 ha^{-1})	18.68 (8.72)	7.92 (2.78)	10.77	0.53	53	12.88
	QMD (cm)	30.44 (6.12)	23.69 (3.94)	6.75	0.14	31	9.22
	Trees ha^{-1}	142 (134)	69 (19)	73.46	0.44	73	138.71
0.81 (ha)	CBD (kg m^{-3})	0.08 (0.06)	0.02 (0.01)	0.05	0.07	54	0.08
	CBH (m)	2.63 (1.09)	6.28 (1.4)	-3.65	-0.51	176	4.17
	TopHt (m)	12.87 (3.51)	13.88 (1.26)	-1.00	0.4	22	3.15
	CC (%)	44.84 (25.28)	50.23 (29.71)	-5.39	0.12	82	34.26
	BA (m^2 ha^{-1})	18.32 (8.26)	7.78 (2.73)	10.55	0.55	53	12.44
	QMD (cm)	30.91(6.66)	23.61 (4.01)	7.3	-0.02	32	10.29
	Trees ha^{-1}	143 (137)	66 (18)	73.93	0.45	74	140.77
1.44 (ha)	CBD (kg m^{-3})	0.08 (0.06)	0.02 (0.01)	0.05	0.01	54	0.08
	CBH (m)	2.57 (1.04)	6.26 (1.35)	-3.7	-0.51	182	4.17
	TopHt (m)	12.70 (3.57)	13.94 1.31)	-1.24	0.46	23	3.20
	CC (%)	45.36 (25.84)	51.68 (29.22)	-6.32	0.11	88	34.75
	BA (m^2 ha^{-1})	18.48 (8.67)	7.92 (2.78)	10.56	0.53	52	12.68
	QMD (cm)	30.36 (6.25)	23.69 (3.94)	6.68	0.15	31	9.23
	Trees ha^{-1}	145 (124)	70 (19)	74.43	0.42	74	131.73
2.25 (ha)	CBD (kg m^{-3})	0.08 (0.06)	0.02 (0.01)	0.06	-0.11	57	0.08
	CBH (m)	2.61 (1.19)	6.25 (1.30)	-3.64	-0.49	186	4.15
	TopHt (m)	12.82 (3.70)	13.97 (1.29)	-1.15	0.49	23	3.24
	CC (%)	47 (24.45)	53.01 (28.31)	-6.01	0.02	79	32.39
	BA (m^2 ha^{-1})	19.40 (9.09)	7.96 (2.69)	11.44	0.54	54	13.61
	QMD (cm)	30.26 (5.93)	23.66 (3.78)	6.6	0.27	29	8.69
	Trees ha^{-1}	144 (134)	70 (18)	74.21	0.46	29	138.98

Table 1.11. LANDFIRE observed – predicted canopy metric summary statistics across increasing map scales from 0.09-2.25 ha. Summary statistics include mean observed fuel metric and (standard deviation), mean predicted LANDFIRE fuel metric and (standard deviation), mean error (ME), correlation coefficient (R), mean absolute percent error (MAPE), and root mean squared error (RMSE). CBD: canopy bulk density; CBH: canopy base height; TopHt: canopy top height; CC: canopy cover.

Map Scale	Canopy Attribute	Mean Observed	Mean Predicted	ME	R	MAPE	RMSE
0.09 (ha)	CBD (kg m^{-3})	0.08 (0.06)	0.08 (0.02)	0.01	0.75	42	0.04
	CBH (m)	2.54 (1.24)	1.1 (0.92)	1.44	0.13	54	1.97
	TopHt (m)	12.82 (3.70)	13.92 (3.17)	-1.11	0.53	24	3.31
	CC (%)	47 (24.45)	39.62 (10.27)	7.38	0.91	30	16.34
0.36 (ha)	CBD (kg m^{-3})	0.08 (0.06)	0.07 (0.02)	0.00	0.85	44	0.04
	CBH (m)	2.59 (1.05)	1.11 (1.11)	1.49	0.36	57	1.86
	TopHt (m)	12.80 (3.57)	14.12 (3.10)	-1.32	0.49	25	3.40
	CC (%)	45.53 (25.47)	38.13 (10.68)	7.40	0.9	33	17.01
0.81 (ha)	CBD (kg m^{-3})	0.08 (0.06)	0.08 (0.02)	0.00	0.86	47	0.04
	CBH (m)	2.63 (1.09)	1.08 (1.10)	1.55	0.4	60	1.91
	TopHt (m)	12.87 (3.51)	14.04 (3.22)	-1.17	0.5	23	3.35
	CC (%)	44.84 (25.28)	38.04 (10.52)	6.8	0.89	31	16.76
1.44 (ha)	CBD (kg m^{-3})	0.08 (0.06)	0.08 (0.02)	0.00	0.85	45	0.04
	CBH (m)	2.57 (1.04)	1.09 (1.11)	1.47	0.33	57	1.87
	TopHt (m)	12.70 (3.57)	14.18 (3.05)	-1.48	0.48	26	3.49
	CC (%)	45.36 (25.84)	38.13 (10.68)	7.24	0.90	33	17.18
2.25 (ha)	CBD (kg m^{-3})	0.08 (0.06)	0.08 (0.02)	0.01	0.84	38	0.04
	CBH (m)	2.61 (1.19)	1.13 (0.98)	1.48	0.21	54	1.96
	TopHt (m)	12.82 (3.70)	14.30 (2.83)	-1.49	0.51	26	3.42
	CC (%)	47 (24.45)	41.63 (12.81)	5.36	0.47	44	20.69

4. DISCUSSION

4.1. Fuel Map Accuracy

The overarching objective of this study was to provide an assessment of bias and error for three nationally available surface and canopy fuel mapping products – LANDFIRE, FCCS, and FastFuels – at five different scales for seven ponderosa pine-dominated sites across the Colorado Front Range. National fuel mapping products are commonly used to address a variety of scientific questions and to support land and fire management decisions, ranging from fuel hazard reduction design (Drury et al., 2014; Valliant and Reinhardt, 2017) and wildfire hazard and risk assessment (Aragoneses and Chuvieco, 2021; Keane et al., 2010; Prichard et al., 2022; Thompson and Calkin, 2011), to real-time fire operational decisions (Maestas et al., 2023; Rapp et al., 2020; Riley et al., 2018; Ryan and Opperman, 2013). Understanding the accuracy of national fuel mapping products is therefore crucial for ensuring that the scientific conclusions, and fire, land management, and public health

decisions based on their use are based on accurate representations of fuel complexes. In this study, I utilized a gridded sampling design and methodologies similar to those used by the US Forest Service Forest Inventory and Analysis program to assess surface and canopy fuel estimates from LANDFIRE, FCCS, and FastFuels at scales from 0.09 to 2.25 ha. Overall, my results indicate that all three mapping products performed poorly regardless of the fuel component, showing systematic biases with mean absolute errors ranging from 36% to 2590%.

The most common operational fire behavior modeling systems used to predict fire type and rate of spread in the United States, including FARSITE (Finney, 1998), FlamMap (Finney, 2006), BehavePlus (Andrews, 2013), and WFDSS (Pence and Zimmerman, 2011), are especially sensitive to estimates of fine surface fuel load, canopy base height, and canopy bulk density. For these critical fuel metrics, the results of this study indicate mean absolute errors from 36% to 140%, suggesting the potential for these mapping products to introduce significant uncertainty in fire behavior modeling predictions. Large errors associated with canopy base height estimates from both LANDFIRE and FastFuels are particularly concerning, as CBH is a critical variable for estimating the transition of surface to crown fire (Hall and Burke, 2006). I found that LANDFIRE underestimated CBH by an average of 1.4 m in Colorado Front Range ponderosa pine-dominated forests, contradicting the findings of Krasnow et al. (2009) and Reeves et al. (2009). Krasnow et al. (2009) reported that LANDFIRE overestimated CBH in mixed conifer forests of the Colorado Front Range, while Reeves et al. (2009) found a similar overestimation of CBH across a range of forest types in multiple western U.S. states. I found that FastFuels overestimated CBH on average by 2.3 m, suggesting it would underpredict crown fire initiation relative to LANDFIRE. Both LANDFIRE and FastFuels have an underestimation bias for canopy bulk density, but FastFuels' bias is considerably stronger than LANDFIRE's. My finding of LANDFIRE's underprediction bias in CBD aligns with previous evaluations by Krasnow et al. (2009) and Reeves et al. (2009). Underestimation of CBD

suggests that both mapping products may underestimate the potential for crown fire spread. LANDFIRE's CBD estimates had a relatively small bias and a strong positive correlation with field data suggesting it may capture relative patterns in canopy bulk density across an area. In contrast, FastFuels estimates were inversely correlated with field data indicating that underprediction in crown bulk density would likely vary in a non-systematic fashion. The effect of biases and errors in canopy fuel metrics on predicted fire behavior and risk assessments across various fire modeling platforms requires further evaluation to determine their combined influence on fire behavior predictions.

Results show that FCCS surface fuel map accuracies varied widely across fuel components with MAPE from 36% to 2590%. FCCS underestimates fine, 10-, and 100-hour surface fuel loads and overestimates 1000-hour, herbaceous, and shrub fuel loads. Additionally, FCCS estimates had a weak positive correlation with observations, whereas fine fuels showed a negative correlation. Underestimates of fine, 10-, and 100-hour fuels by FCCS observed in this study are consistent with those of Hyde et al. (2015) who sampled mixed conifer forests in Idaho, but conflict with Keane et al. (2013) who utilized FIA fuels data across diverse forest types in eight western U.S. states for comparison However, my finding that FCCS overestimates 1000-hr, herbaceous, and shrub fuel loads are consistent with Keane et al. (2015). Hyde et al. (2015) also found significantly greater predicted herbaceous fuel loads from FCCS but did not find differences in either 1000-hr or shrub loadings for their sites in Idaho. Although this study indicates that FCCS fuel load errors are influenced by topography and forest structure, these factors were weak explanatory variables. Further research assessing errors across forest types, structures, and disturbance histories – along with productivity and decomposition gradients and other potential error sources, such as remote sensing data quality and model calibration constraints – is needed to help develop a mechanistic understanding of surface fuel map errors.

Unlike FCCS and canopy fuel maps, the FBFM40 fuel models have not been previously evaluated for their accuracy in representing surface fuel component loadings. This is largely because the standard fire behavior fuel models were designed to predict attributes of fire behavior using the Rothermel (1972) model rather than to replicate actual fuel loads (Reeves et al., 2009; Scott and Burgan, 2005). Nonetheless, several recent studies have utilized standard fire behavior fuel models – including FastFuels (Marcozzi et al., 2024) – to represent surface fuels for use in next-generation models such as QUIC-Fire, FIRETEC, and WFDS (Linn, 2020; Linn et al., 2002; Mell et al., 2007; Mell et al., 2010). I observed large errors in the FBFM40 surface fuel load estimates across fuel components, ranging from 61% to 1630% MAPE. Fuel loadings for all surface fuel components were overestimated except for herbaceous fuels, which were slightly underestimated relative to field estimates. Additionally, FBFM40 had moderate to strong positive correlations with measured herbaceous and fine fuels, two of the most important fuel components in fire spread prediction. Several possibilities could explain the FBFM40 errors and biases identified in this study. First, 90% of sampling locations were represented by just four FBFM40 models, limiting the amount of variation that can be captured by the fuel map. Another source of error could arise from the reliance on shrub and herbaceous-dominated fuel models during map development to overcome known underprediction biases associated with common U.S. fire behavior modeling systems (Cruz and Alexander, 2010; 2013). A previous Colorado Front Range study found that fire behavior predictions in FARSITE with LANDFIRE surface fuel maps were less accurate than those developed more locally (Krasnow et al., 2009). Unfortunately, understanding the consequences of surface fuel loading errors identified in this study on fire spread predictions is difficult in part because this study does not have concurrent measures and error estimates of fuel bed depth which is a required input to many fire behavior spread models. However, I would expect that given the low fuel loads at these sites, overestimates in fine woody debris and shrub fuel loadings would result in increased surface

fire rates of spread and intensities given all other parameters being equal. Further, the ability of FBFM40 to capture the general trend in herbaceous and fine fuel loading suggests stronger linkages to expected fire behavior compared to the negative correlation for predicted FCCS fine fuels. Further studies are needed to understand errors in fuel bed depth and the sensitivity of various modeling platforms to uncertainties and biases in surface fuel load and depth.

Despite my original expectation that error and bias would improve with increasing spatial scales (0.09 ha to 2.25 ha), I found consistent errors and biases for all fuel components across scales. Although these results were counter to several previous studies in other disciplines (Comber and Harris, 2022; Hu et al., 2024), Fremgen-Tarantino et al. (2021) also found limited interactions between fuel map accuracy and map scale up to 5 km in Idaho and Wyoming sagebrush ecosystems. Previous studies in ponderosa pine-dominated ecosystems suggest that most surface fuel components vary at scales of less than 2 m (Vakili et al., 2016), with canopy fuels being described as a matrix of individuals, openings, and various size tree groups (Ziegler et al., 2014), suggesting that a high degree of variability exists within the smallest 0.09 ha pixel used in our assessment. The large within-pixel variability in surface and canopy fuel loading likely contributed to high errors associated with the fuel mapping products and a lack of scale effect on error and bias. Although our study did not observe an interaction between map scale and accuracy, it is important to note that our evaluation focused on relatively fine scales. Further research should investigate coarser, functional scales – ranging from treatment units (i.e., > 30 ha) to campaign wildfires (i.e., > 40,000 ha) – to assess not just the biases and errors but the implications on fire behavior predictions and decision-making.

4.2. Pathways to Improve Fuel Mapping Efforts

A primary challenge in the development of accurate, broad-scale fuel maps stems from the remarkable spatial variability of wildland fuels. Continuous interactions between environmental

factors (e.g., climate and topography), ecological processes (e.g., deposition, decomposition, and disturbance), and strand structure result in dynamic fuel complexes, with individual surface fuel components and canopy fuel metrics exhibiting significant spatial variability at relatively fine scales (Keane, 2016; Keane et al., 2012; Vakili et al., 2016). Ideally, to effectively capture the variance of each fuel metric, the most appropriate sampling resolution should correspond to the spatial autocorrelation of that fuel metric (e.g., resolutions of 1-2 m for fine fuels and up to approximately 160 m for coarse woody fuels). However, current fuel mapping approaches primarily rely on nationally consistent remotely sensed data from Landsat with a 30 m resolution. Although the continuity of the long-term Landsat mission is attractive because it can be used to describe changes in the environment since the late 1980s, the resolution may be too coarse to effectively capture the fine-scale variability of surface fuels which is largely driven by forest density and canopy cover (Hoffman et al., 2023). This mismatch between mapping resolution and the spatial variability of individual fuel metrics contributes to the large errors observed among these national fuel mapping products.

Beyond resolution challenges, the reliance on passive optical remote sensors like Landsat further limits fuel mapping accuracy, as spectral signatures only reliably capture forest canopies, with limited information about the forest understory. Recent advancements in remote sensing technologies leveraging Light Detection and Ranging (LiDAR) and Synthetic Aperture Radar (SAR) provide a promising avenue to address limitations associated with both spatial resolution and passive remote sensing. Because these active sensors provide direct observations of canopy structure, they have been shown to improve estimates of CBH, canopy height, and canopy cover compared to passive satellite observations (Arkin et al., 2021; Chamberlain et al., 2021; Engelstad et al., 2019; Moran et al., 2020). These active sensors have also been shown to improve surface fuel estimation through refined vegetation type mapping and classification (Hoffrén et al., 2023; Leite et

al., 2024; Smith et al., 2020). By integrating data from multiple sensors (e.g., Sentinel, GEDI, ATLAS, PRISMA, Amazonia-1), fuels data can be captured at a range of resolutions better suited to the variability of individual fuel components. Integrating sensors like GEDI's satellite-based LiDAR and Sentinel-1's combination of SAR and passive optical data has provided improved canopy height and biomass prediction accuracy globally compared to estimates from passive optical sensors alone (Guo et al., 2023) and therefore should be explored for the potential to enhance fuel map accuracy. While improvements in canopy fuel metrics have been demonstrated by integrating passive and active sensors, less is known about whether these techniques would improve surface fuel predictions.

Directly predicting surface fuel component loadings could further improve fuel map accuracy by overcoming the limitations of generalized fuelbeds, which rely on the classification of a finite set of values used for fire behavior prediction. Individual fuel component loadings could be effectively estimated by leveraging mechanistic relationships between canopy structure attributes (e.g., basal area, canopy cover, canopy density) and surface fuels (Dell et al., 2017; Jakubowski et al., 2013; Lin et al., 2021; Lin et al., 2016; Lydersen et al., 2015; Nguyen et al., 2024; Siegart et al., 2020) with improved canopy structure covariates and increased direct observations of surface fuels provided by active sensors (Stefanidou et al., 2020). Emerging modeling techniques, such as constrained multivariate regression models, could integrate these advancements to simultaneously predict individual fuel components (Anderson et al., 2019; Ascari et al., 2024; Cook et al., 2024; Dray et al., 2012; Sîrbu et al., 2021) while maintaining total surface fuel loading to enable more reliable surface fuel estimates across landscapes.

While active sensors offer a promising solution for improving fuel mapping, fully integrating these technologies will take time. In the short term, fuel maps could be improved using double sampling techniques to correct bias and enhance accuracy at regional to landscape scales.

Previous efforts have significantly reduced biases by using a secondary sample to calibrate broad-extent remote sensing products for local applications (Yung-Han et al., 2020). Local fuel loading estimates from field inventories, terrestrial LiDAR, and uncrewed aerial system-derived data could all be useful for double sample correction of national fuel maps. Implementing a regression-based double sample correction requires the fuel map errors to linearly scale with the local estimate (Burkhart et al., 2019, so this might only be possible for the fuel map metrics where error was significantly related to observed fuel load (Table 1.7).

Another challenge in accurately mapping wildland fuels stems from their vast temporal variability (Keane, 2016). Currently, LANDFIRE updates FBFM40 and canopy attribute maps every 1-3 years (with plans for future annual updates), FCCS is updated every four years, and TreeMap – the canopy data supporting FastFuels – has been released only once in 2016. Given the dynamic nature of fuels, particularly in areas undergoing rapid changes due to wildfire (Stevens-Rumann et al., 2020), bark beetle infestations (Jenkins et al., 2008), or disease (Hoffman et al., 2007), and management practices including hazardous fuel reduction and restoration treatments (Stephens et al., 2012), the infrequency of map updates cannot adequately capture temporal changes in fuel complexes, likely contributing to mapping errors. Integrating existing Landsat-derived disturbance products (i.e., Dubayah et al., 2020; Eidenshink et al., 2007 Kennedy et al., 2010) could improve alignment between fuel maps and current conditions. Furthermore, as these national fuel mapping products continue to evolve, they must also incorporate more rigorous error tracking to enhance reliability. NASA's Carbon Monitoring System (Hurtt et al., 2014; Hurtt et al., 2022) provides a model for systematically quantifying and communicating uncertainty – an approach that could provide more reliable and actionable fuel data for fire and land management applications.

5. CONCLUSIONS

Substantial errors and biases, like those observed in our evaluation, may have significant implications for the use of national fuel mapping products to inform fire management, public safety, and ecosystem health decisions. Inaccuracies in fuel maps are particularly critical for decision-makers in the context of initiatives like the USFS Wildfire Crisis Strategy, which has allocated $170.4 million for the implementation of forest treatments across the Colorado Front Range (USDA Forest Service, 2022). This study indicates that estimates of key fuel complex metrics including fine surface fuel loads, canopy base height, and canopy bulk density from national fuel mapping products including LANDFIRE exhibited large errors and systematic biases. For example, LANDFIRE's underestimation of CBH would lead to increased prediction of crown fire initiation, however, underestimates of CBD would lead to underprediction of crown fire spread. Conversely, FastFuels' overestimation of CBH alongside underestimates of CBD would likely lead to underpredictions of both crown fire initiation and spread. Surface fuel load estimates are also a critical input for predictions of wildfire smoke and emissions (Drury et al., 2014; Larkin et al., 2012; Prichard et al., 2019) – a key concern because fine particulate matter in wildfire smoke poses serious risks to public health (Aguilera et al., 2021; Gould et al., 2024; Reisen et al., 2015). I found that FCCS, the primary fuel map employed for these forecasts, grossly overestimated 1000-hour and shrub fuel loads. These overestimates could inflate smoke and emissions predictions beyond permittable thresholds, preventing managers from implementing prescribed fires aimed at reducing surface fuel loads (Liu et al., 2017).

Although my assessment, along with previous studies, has demonstrated substantial errors and biases associated with fine-scale estimates of fuels complex from LANDFIRE, FCCS, and FastFuels, these national fuel mapping data products remain valuable tools for characterizing and assessing fuels across broad spatial scales and ownerships (Keane et al., 2013). Advances in

remote sensing and modeling technologies suggest that there are opportunities to improve fuel mapping accuracy and reliability. However, the diffusion and adoption of new approaches across land management agencies is a complex process that involves learning, adaptation, and integration of technology into decision-making processes. Until new fuel mapping methods are more widely available and utilized, there is a need to continue to quantify and consider uncertainties in existing fuel mapping products.

REFERENCES

Agee, J. K. (1996, January). The influence of forest structure on fire behavior. In *Proceedings of the 17th annual forest vegetation management conference* (pp. 52-68).

Ager, A. A., Vaillant, N. M., & Finney, M. A. (2011). Integrating fire behavior models and geospatial analysis for wildland fire risk assessment and fuel management planning. *Journal of Combustion*, *2011*(1), 572452.

Aguilera, R., Corringham, T., Gershunov, A., & Benmarhnia, T. (2021). Wildfire smoke impacts respiratory health more than fine particles from other sources: observational evidence from Southern California. *Nature communications*, *12*(1), 1493.

Åkerblom, M., & Kaitaniemi, P. (2021). Terrestrial laser scanning: a new standard of forest measuring and modelling?. *Annals of Botany*, *128*(6), 653-662.

Albini, F. A. (1996). Iterative solution of the radiation transport equations governing spread of fire in wildland fuel. *Combustion, Explosion and Shock Waves*, *32*(5), 534-543.

Anderson, H. E. (1982). Aids to determining fuel models for estimating fire behavior. *The Bark Beetles, Fuels, and Fire Bibliography*, 143.

Anderson, M. J., de Valpine, P., Punnett, A., & Miller, A. E. (2019). A pathway for multivariate analysis of ecological communities using copulas. *Ecology and evolution*, *9*(6), 3276-3294.

Andrews, P. L. (2013). Current status and future needs of the BehavePlus Fire Modeling System. *International Journal of Wildland Fire*, *23*(1), 21-33.

Andrews, P. L., Bevins, C. D., & Seli, R. C. (2005). BehavePlus fire modeling system, version 4.0: User's Guide. *Gen. Tech. Rep. RMRS-GTR-106 Revised. Ogden, UT: Department of Agriculture, Forest Service, Rocky Mountain Research Station. 132p.*, *106*.

Atchley, A. L., Linn, R., Jonko, A., Hoffman, C., Hyman, J. D., Pimont, F., ... & Middleton, R. S. (2021). Effects of fuel spatial distribution on wildland fire behaviour. *International journal of wildland fire*, *30*(3), 179-189.

Aragoneses, E., & Chuvieco, E. (2021). Generation and mapping of fuel types for fire risk assessment. *Fire*, *4*(3), 59.

Arkin, J., Coops, N. C., Daniels, L. D., & Plowright, A. (2021). Estimation of vertical fuel layers in tree crowns using high density lidar data. *Remote Sensing*, *13*(22), 4598.

Arroyo, L. A., Pascual, C., & Manzanera, J. A. (2008). Fire models and methods to map fuel types: The role of remote sensing. *Forest ecology and management*, *256*(6), 1239-1252.

Ascari, R., Di Brisco, A. M., Migliorati, S., & Ongaro, A. (2024). A Multivariate Mixture Regression Model for Constrained Responses. *Bayesian Analysis*, *19*(2), 377-405.

Brown, J. K. (1974). Handbook for inventorying downed woody material. Gen. Tech. Rep. INT-16. Ogden, UT: US Department of Agriculture, Forest Service, Intermountain Forest and Range Experiment Station. 24 p., 16.

Brown, J. K. (1978). *Weight and density of crowns of Rocky Mountain conifers* (Vol. 197). Department of Agriculture, Forest Service, Intermountain Forest and Range Experiment Station.

Brown, J. K., & See, T. E. (1981). Downed dead woody fuel and biomass in the northern Rocky Mountains. General Technical Report INT-GTR-117. Ogden, UT: USDA Forest Service Intermountain Forest and Range Experiment Station. 48 p.

Brown, S., Gillespie, A. J., & Lugo, A. E. (1989). Biomass estimation methods for tropical forests with applications to forest inventory data. *Forest science*, *35*(4), 881-902.

Burgan, R. E. (1987). *Concepts and interpreted examples in advanced fuel modeling* (Vol. 238). US Department of Agriculture, Forest Service, Intermountain Research Station.

Burgan, R. E., & Rothermel, R. C. (1984). BEHAVE: fire behavior prediction and fuel modeling system--FUEL subsystem. General Technical Report INT-167. Ogden, UT: U. S. Department of Agriculture, Forest Service, Intermountain Forest and Range Experiment Station. 126 p.

Burkhart, H. E., Avery, T. E., Bullock, B. P. (2019). Forest Measurements, 6th Edition. Waveland Press, Long Grove, IL, United States.

Chamberlain, C. P., Meador, A. J. S., & Thode, A. E. (2021). Airborne lidar provides reliable estimates of canopy base height and canopy bulk density in southwestern ponderosa pine forests. *Forest Ecology and Management*, *481*, 118695.

Chave, J., Andalo, C., Brown, S., Cairns, M. A., Chambers, J. Q., Eamus, D., ... & Yamakura, T. (2005). Tree allometry and improved estimation of carbon stocks and balance in tropical forests. *Oecologia*, *145*, 87-99.

Chave, J., Réjou-Méchain, M., Búrquez, A., Chidumayo, E., Colgan, M. S., Delitti, W. B., ... & Vieilledent, G. (2014). Improved allometric models to estimate the aboveground biomass of tropical trees. *Global change biology*, *20*(10), 3177-3190.

Che Azmi, N. A., Mohd Apandi, N., & A. Rashid, A. S. (2021). Carbon emissions from the peat fire problem—a review. *Environmental Science and Pollution Research*, *28*, 16948-16961.

Chuvieco, E. (2020). *Fundamentals of satellite remote sensing: An environmental approach*. CRC press.

Chuvieco, E., & Congalton, R. G. (1989). Application of remote sensing and geographic information systems to forest fire hazard mapping. *Remote sensing of Environment*, *29*(2), 147-159.

Chuvieco, E., Salas, J., & Vega, C. (1997). Remote sensing and GIS for long-term fire risk mapping. *A review of remote sensing methods for the study of large wildland fires*, 91-108.

Comber, A., & Harris, P. (2022). The importance of scale and the MAUP for robust ecosystem service evaluations and landscape decisions. *Land*, *11*(3), 399.

Cook, R. D., Forzani, L., & Liu, L. (2024). Envelopes for multivariate linear regression with linearly constrained coefficients. *Scandinavian Journal of Statistics*, *51*(2), 429-446.

Countryman, C. M. (1972). *The fire environment concept*. Pacific Southwest Forest and Range Experiment Station.

Cruz, M. G., & Alexander, M. E. (2010). Assessing crown fire potential in coniferous for

Cruz, M. G., & Alexander, M. E. (2013). Uncertainty associated with model predictions of surface and crown fire rates of spread. *Environmental Modelling & Software*, *47*, 16-28.

Cruz, M. G., Alexander, M. E., & Wakimoto, R. H. (2003). Assessing canopy fuel stratum characteristics in crown fire prone fuel types of western North America. *International Journal of Wildland Fire*, *12*(1), 39-50.

Cruz, M. G., Alexander, M. E., & Wakimoto, R. H. (2005). Development and testing of models for predicting crown fire rate of spread in conifer forest stands. *Canadian Journal of Forest Research*, *35*(7), 1626-1639.

Daubenmire, R. F. (1959). A canopy-coverage method of vegetational analysis. Northwest Science, 33, 43-64.

DeCastro, A. L., Juliano, T. W., Kosović, B., Ebrahimian, H., & Balch, J. K. (2022). A computationally efficient method for updating fuel inputs for wildfire behavior models using sentinel imagery and random forest classification. *Remote Sensing*, *14*(6), 1447.

Dell, J. E., Richards, L. A., O'Brien, J. J., Loudermilk, E. L., Hudak, A. T., Pokswinski, S. M., ... & Dyer, L. A. (2017). Overstory-derived surface fuels mediate plant species diversity in frequently burned longleaf pine forests. *Ecosphere*, *8*(10), e01964.

Djomo, A. N., & Chimi, C. D. (2017). Tree allometric equations for estimation of above, below and total biomass in a tropical moist forest: Case study with application to remote sensing. *Forest Ecology and Management*, *391*, 184-193.

Dixon, Gary E. comp. 2002 (Revised February 2013). Essential FVS: a user's guide to the Forest Vegetation Simulator. Internal Rep. Fort Collins, CO: USDA Forest Service, Forest Management Service Center. 226p.

Domingo, D., de la Riva, J., Lamelas, M. T., García-Martín, A., Ibarra, P., Echeverría, M., & Hoffrén, R. (2020). Fuel type classification using airborne laser scanning and Sentinel 2 data in Mediterranean forest affected by wildfires. *Remote Sensing*, *12*(21), 3660.

Donager, J. J., Sánchez Meador, A. J., & Blackburn, R. C. (2021). Adjudicating perspectives on forest structure: how do airborne, terrestrial, and mobile lidar-derived estimates compare?. *Remote Sensing*, *13*(12), 2297.

Dos Santos, A. C., da Rocha Montenegro, S., Ferreira, M. C., Barradas, A. C. S., & Schmidt, I. B. (2021). Managing fires in a changing world: Fuel and weather determine fire behavior and safety in the neotropical savannas. *Journal of environmental management*, *289*, 112508.

Dray, S., Pélissier, R., Couteron, P., Fortin, M. J., Legendre, P., Peres-Neto, P. R., ... & Wagner, H. H. (2012). Community ecology in the age of multivariate multiscale spatial analysis. *Ecological Monographs*, *82*(3), 257-275.

Drury, S. A., Larkin, N. S., Strand, T. T., Huang, S., Strenfel, S. J., Banwell, E. M., ... & Raffuse, S. M. (2014). Intercomparison of fire size, fuel loading, fuel consumption, and smoke emissions estimates on the 2006 Tripod Fire, Washington, USA. *Fire Ecology*, *10*, 56-83.

Dubayah, R., Blair, J. B., Goetz, S., Fatoyinbo, L., Hansen, M., Healey, S., ... & Silva, C. (2020). The Global Ecosystem Dynamics Investigation: High-resolution laser ranging of the Earth's forests and topography. *Science of remote sensing*, *1*, 100002.

Duff, T. J., Cawson, J. G., & Penman, T. D. (2019). Determining burnability: Predicting completion rates and coverage of prescribed burns for fuel management. *Forest ecology and management*, *433*, 431-440.

Eidenshink, J., Schwind, B., Brewer, K., Zhu, Z. L., Quayle, B., & Howard, S. (2007). A project for monitoring trends in burn severity. *Fire ecology*, *3*, 3-21.

Engelstad, P. S., Falkowski, M., Wolter, P., Poznanovic, A., & Johnson, P. (2019). Estimating canopy fuel attributes from low-density LiDAR. *Fire*, *2*(3), 38.

ESRI. (2023). ArcGIS Desktop: Release 3.2.0. Redlands, CA: Environmental Systems Research Institute

FastFuels Python SDK - PyPI. (n.d.). Python Software Foundation. Retrieved from https://pypi.org/

Finney, M. A. (1998). *FARSITE, Fire Area Simulator--model development and evaluation* (No. 4). US Department of Agriculture, Forest Service, Rocky Mountain Research Station.

Finney, M. A. (2006). An overview of FlamMap fire modeling capabilities. In *In: Andrews, Patricia L.; Butler, Bret W., comps. 2006. Fuels Management-How to Measure Success: Conference Proceedings. 28-30 March 2006; Portland, OR. Proceedings RMRS-P-41. Fort Collins, CO: US Department of Agriculture, Forest Service, Rocky Mountain Research Station. p. 213-220* (Vol. 41).

Forghani, A., Cechet, B., Radke, J., Finney, M., & Butler, B. (2007, July). Applying fire spread simulation over two study sites in California lessons learned and future plans. In *2007 IEEE International Geoscience and Remote Sensing Symposium* (pp. 3008-3013). IEEE.

Fremgen-Tarantino, M. R., Olsoy, P. J., Frye, G. G., Connelly, J. W., Krakauer, A. H., Patricelli, G. L., & Forbey, J. S. (2021). Assessing accuracy of GAP and LANDFIRE land cover datasets in winter habitats used by greater sage-grouse in Idaho and Wyoming, USA. *Journal of Environmental Management*, *280*, 111720.

Gould, C. F., Heft-Neal, S., Johnson, M., Aguilera, J., Burke, M., & Nadeau, K. (2024). Health effects of wildfire smoke exposure. *Annual Review of Medicine*, *75*(1), 277-292.

Gould, N. P., Pomara, L. Y., Nepal, S., Goodrick, S. L., & Lee, D. C. (2023). Mapping firescapes for wild and prescribed fire management: A landscape classification approach. *Land*, *12*(12), 2180.

Gouma, V., & Chronopoulou-Sereli, A. (1998). Wildland fire danger zoning–a methodology. *International Journal of Wildland Fire*, *8*(1), 37-43.

Guo, Q., Du, S., Jiang, J., Guo, W., Zhao, H., Yan, X., ... & Xiao, W. (2023). Combining GEDI and sentinel data to estimate forest canopy mean height and aboveground biomass. *Ecological Informatics*, *78*, 102348.

Hall, S. A., & Burke, I. C. (2006). Considerations for characterizing fuels as inputs for fire behavior models. *Forest Ecology and Management*, *227*(1-2), 102-114.

Hoffman, C., Mathiasen, R., & Sieg, C. H. (2007). Dwarf mistletoe effects on fuel loadings in ponderosa pine forests in northern Arizona. *Canadian Journal of Forest Research*, *37*(3), 662-670.

Hoffman, C. M., Ziegler, J. P., Tinkham, W. T., Hiers, J. K., & Hudak, A. T. (2023). A comparison of four spatial interpolation methods for modeling fine-scale surface fuel load in a mixed conifer forest with complex terrain. *Fire*, *6*(6), 216.

Hoffrén, R., Lamelas, M. T., de la Riva, J., Domingo, D., Montealegre, A. L., García-Martín, A., & Revilla, S. (2023). Assessing GEDI-NASA system for forest fuels classification using machine learning techniques. *International Journal of Applied Earth Observation and Geoinformation*, *116*, 103175.

Hu, Y., Fernandez-Anez, N., Smith, T. E., & Rein, G. (2018). Review of emissions from smouldering peat fires and their contribution to regional haze episodes. *International Journal of Wildland Fire*, *27*(5), 293-312.

Hu, Z., Chu, Y., Zhang, Y., Zheng, X., Wang, J., Xu, W., ... & Wu, G. (2024). Scale matters: How spatial resolution impacts remote sensing based urban green space mapping?. *International Journal of Applied Earth Observation and Geoinformation*, *134*, 104178.

Hungerford, R. D., Frandsen, W. H., & Ryan, K. C. (1995). Ignition and burning characteristics of organic soils. In *Tall Timbers Fire Ecology Conference* (Vol. 19, pp. 78-91).

Hurtt, G. C., Andrews, A., Bowman, K., Brown, M. E., Chatterjee, A., Escobar, V., ... & Tian, H. (2022). The NASA carbon monitoring system phase 2 synthesis: scope, findings, gaps and recommended next steps. *Environmental Research Letters*, *17*(6), 063010.

Hurtt, G., Wickland, D., Jucks, K., Bowman, K., Brown, M. E., Duren, R. M., ... & Verdy, A. (2014, October). *NASA carbon monitoring system: prototype monitoring, reporting, and verification*.

Hyde, J., Strand, E. K., Hudak, A. T., & Hamilton, D. (2015). A case study comparison of LANDFIRE fuel loading and emissions generation on a mixed conifer forest in northern Idaho, USA. *Fire Ecology*, *11*, 108-127.

Hudak, A. T., Kato, A., Bright, B. C., Loudermilk, E. L., Hawley, C., Restaino, J. C., ... & Weise, D. R. (2020). Towards spatially explicit quantification of pre-and postfire fuels and fuel consumption from traditional and point cloud measurements. *Forest Science*, *66*(4), 428-442.

Jakubowksi, M. K., Guo, Q., Collins, B., Stephens, S., & Kelly, M. (2013). Predicting surface fuel models and fuel metrics using Lidar and CIR imagery in a dense, mountainous forest. *Photogrammetric Engineering & Remote Sensing*, *79*(1), 37-49.

Jenkins, M. J., Hebertson, E., Page, W., & Jorgensen, C. A. (2008). Bark beetles, fuels, fires and implications for forest management in the Intermountain West. *Forest Ecology and Management*, *254*(1), 16-34.

Keane, R. E., & Dickinson, L. J. (2007). *The photoload sampling technique: estimating surface fuel loadings from downward-looking photographs of synthetic fuelbeds*. US Department of Agriculture, Forest Service, Rocky Mountain Research Station, General Technical Report. RMRS-GTR-190.

Keane, R. E. (2015). *Wildland fuel fundamentals and applications* (No. 11904). Cham, Switzerland: Springer International Publishing.

Keane, R. E. (2016). Spatiotemporal variability of wildland fuels in US northern Rocky Mountain forests. Forests, 7(7), 129.

Keane, R. E., Burgan, R., & van Wagtendonk, J. (2001). Mapping wildland fuels for fire management across multiple scales: Integrating remote sensing, GIS, and biophysical modeling. *International Journal of Wildland Fire*, *10*(4), 301-319.

Keane, R. E., Drury, S. A., Karau, E. C., Hessburg, P. F., & Reynolds, K. M. (2010). A method for mapping fire hazard and risk across multiple scales and its application in fire management. *Ecological Modelling*, *221*(1), 2-18.

Keane, R. E., Gray, K., & Bacciu, V. (2012). Spatial variability of wildland fuel characteristics in northern Rocky Mountain ecosystems. Res. Pap. RMRS-RP-98. Fort Collins, CO: US Department of Agriculture, Forest Service, Rocky Mountain Research Station. 56 p., 98.

Keane, R. E., Gray, K. (2013). Comparing three sampling techniques for estimating fire woody down dead biomass. *International Journal of Wildland Fire, 22*, 1093-1107.

Keane, R. E., Herynk, J. M., Toney, C., Urbanski, S. P., Lutes, D. C., & Ottmar, R. D. (2013). Evaluating the performance and mapping of three fuel classification systems using Forest Inventory and Analysis surface fuel measurements. *Forest Ecology and Management*, *305*, 248-263.

Keane, R. E., & Reeves, M. (2011). Use of expert knowledge to develop fuel maps for wildland fire management. In *Expert knowledge and its application in landscape ecology* (pp. 211-228). New York, NY: Springer New York.

Kennedy, R. E., Yang, Z., & Cohen, W. B. (2010). Detecting trends in forest disturbance and recovery using yearly Landsat time series: 1. LandTrendr—Temporal segmentation algorithms. *Remote Sensing of Environment*, *114*(12), 2897-2910.

Krasnow, K., Schoennagel, T., & Veblen, T. T. (2009). Forest fuel mapping and evaluation of LANDFIRE fuel maps in Boulder County, Colorado, USA. *Forest Ecology and Management*, *257*(7), 1603-1612.

Kreye, J. K., Varner, J. M., & Kobziar, L. N. (2020). Long-duration soil heating resulting from forest floor duff smoldering in longleaf pine ecosystems. *Forest Science*, *66*(3), 291-303.

LANDFIRE. (2020). Fuel Characteristic Classification System Fuelbeds, LANDFIRE 2.2.0, U.S. Department of the Interior, Geological Survey, and U.S. Department of Agriculture. Accessed 29, November, (2023) at http://www.landfire/viewer

LANDFIRE. (2023a). 40 Fire Behavior Fuel Models-Scott/Burgan, LANDFIRE 2.4.0, U.S. Department of the Interior, Geological Survey, and U.S. Department of Agriculture. Accessed 29, November, (2023) at http://www.landfire/viewer.

LANDFIRE. (2023b). Existing Vegetation Cover (EVC) Conus, LANDFIRE 2.4.0, U.S. Department of the Interior, Geological Survey, and U.S. Department of Agriculture.

LANDFIRE. (2023c). Existing Vegetation Height (EVH) Conus, LANDFIRE 2.4.0, U.S. Department of the Interior, Geological Survey, and U.S. Department of Agriculture.

LANDFIRE. (2023d). Existing Vegetation Type (EVT) Conus, LANDFIRE 2.4.0, U.S. Department of the Interior, Geological Survey, and U.S. Department of Agriculture.LANDFIRE. (2023a). Forest Canopy Base Height, LANDFIRE 2.4.0, U.S. Department of the Interior, Geological Survey, and U.S. Department of Agriculture. Accessed 7, March, (2024) at http://www.landfire/viewer

LANDFIRE. (2023e). Forest Canopy Base Height, LANDFIRE 2.4.0, U.S. Department of the Interior, Geological Survey, and U.S. Department of Agriculture. Accessed 7, March, (2024) at http://www.landfire/viewer

LANDFIRE. (2023f). Forest Canopy Bulk Density, LANDFIRE 2.4.0, U.S. Department of the Interior, Geological Survey, and U.S. Department of Agriculture. Accessed 7, March, (2024) at http://www.landfire/viewer

LANDFIRE. (2023g). Forest Canopy Cover, LANDFIRE 2.4.0, U.S. Department of the Interior, Geological Survey, and U.S. Department of Agriculture. Accessed 7, March, (2024) at http://www.landfire/viewer

LANDFIRE. (2024, December – last update). [Homepage of the LANDFIRE Project, U.S. Department of Interior], [Online]. Available: https://www.landfire.gov

Larkin, N. K., Strand, T. M., Drury, S. A., Raffuse, S. M., Solomon, R. C., O'Neill, S. M., ... & Hafner, H. R. (2012). Phase 1 of the Smoke and Emissions Model Intercomparison Project (SEMIP): Creation of SEMIP and evaluation of current models.

Larkin, N. K., Raffuse, S. M., & Strand, T. M. (2014). Wildland fire emissions, carbon, and climate: US emissions inventories. Forest Ecology and Management, 317, 61-69.

Leite, R. V., Amaral, C., Neigh, C. S., Cosenza, D. N., Klauberg, C., Hudak, A. T., ... & Silva, C. A. (2024). Leveraging the next generation of spaceborne Earth observations for fuel monitoring and wildland fire management. *Remote Sensing in Ecology and Conservation*.

Lin, C., Ma, S. E., Huang, L. P., Chen, C. I., Lin, P. T., Yang, Z. K., & Lin, K. T. (2021). Generating a baseline map of surface fuel loading using stratified random sampling inventory data through cokriging and multiple linear regression methods. *Remote Sensing*, *13*(8), 1561.

Lin, C., Tsogt, K., & Zandraabal, T. (2016). A decompositional stand structure analysis for exploring stand dynamics of multiple attributes of a mixed-species forest. *Forest Ecology and Management*, *378*, 111-121.

Linn, R. R., Goodrick, S. L., Brambilla, S., Brown, M. J., Middleton, R. S., O'Brien, J. J., & Hiers, J. K. (2020). QUIC-fire: A fast-running simulation tool for prescribed fire planning. *Environmental Modelling & Software*, *125*, 104616.

Linn, R., Reisner, J., Colman, J. J., & Winterkamp, J. (2002). Studying wildfire behavior using FIRETEC. *International journal of wildland fire*, *11*(4), 233-246.

Liu, Y., Kochanski, A., Baker, K. R., Mell, W., Linn, R., Paugam, R., ... & McNamara, D. (2019). Fire behaviour and smoke modelling: model improvement and measurement needs for next-generation smoke research and forecasting systems. *International journal of wildland fire*, *28*(8), 570-588.

Liu, X., Huey, L. G., Yokelson, R. J., Selimovic, V., Simpson, I. J., Müller, M., ... & Wolfe, G. M. (2017). Airborne measurements of western US wildfire emissions: Comparison with prescribed burning and air quality implications. Journal of Geophysical Research: Atmospheres, 122(11), 6108-6129.

Loudermilk, E. L., Hiers, J. K., & O'Brien, J. J. (2017). The role of fuels for understanding fire behavior and fire effects. In *Ecological restoration and management of longleaf pine forests* (pp. 107-122). CRC Press.

Loudermilk, E. L., Pokswinski, S., Hawley, C. M., Maxwell, A., Gallagher, M. R., Skowronski, N. S., ... & Hiers, J. K. (2023). Terrestrial laser scan metrics predict surface vegetation biomass and consumption in a frequently burned southeastern US ecosystem. *Fire*, *6*(4), 151.

Loudermilk, E. L., Singhania, A., Fernandez, J. C., Hiers, J. K., O'Brien, J. J., Cropper Jr, W. P., ... & Mitchell, R. J. (2007). Application of ground-based LIDAR for fine-scale forest fuel modeling. *USDA Forest Service Proceedings RMRS-P-46CD*, *662*, 515-523.

Lutes, D. C., Keane, R. E., Caratti, J. F., Key, C. H., Benson, N. C., Sutherland, S., & Gangi, L. J. (2006). FIREMON: Fire effects monitoring and inventory system. *Gen. Tech. Rep. RMRS-GTR-164. Fort Collins, CO: US Department of Agriculture, Forest Service, Rocky Mountain Research Station. 1 CD.*, *164*.

Lydersen, J. M., Collins, B. M., Brooks, M. L., Matchett, J. R., Shive, K. L., Povak, N. A., ... & Smith, D. F. (2017). Evidence of fuels management and fire weather influencing fire severity in an extreme fire event. *Ecological Applications*, *27*(7), 2013-2030.

Lydersen, J. M., Collins, B. M., Knapp, E. E., Roller, G. B., & Stephens, S. (2015). Relating fuel loads to overstorey structure and composition in a fire-excluded Sierra Nevada mixed conifer forest. *International Journal of Wildland Fire*, *24*(4), 484-494.

Maestas, J. D., Smith, J. T., Allred, B. W., Naugle, D. E., Jones, M. O., O'Connor, C., ... & Olsen, A. C. (2023). Using dynamic, fuels-based fire probability maps to reduce large wildfires in the Great Basin. *Rangeland Ecology & Management*, *89*, 33-41.

Marcozzi, A., Wells, L., Parsons, R., Mueller, E., Linn, R., & Hiers, J. K. (2024). FastFuels: Advancing wildland fire modeling with high-resolution 3D fuel data and data assimilation. *Environmental Modelling & Software*, 106214.

Marsha, A. L., & Larkin, N. K. (2022). Evaluating satellite fire detection products and an ensemble approach for estimating burned area in the United States. *Fire*, *5*(5), 147.

McCarley, T. R., Hudak, A. T., Restaino, J. C., Billmire, M., French, N. H., Ottmar, R. D., ... & Volkamer, R. (2022). A comparison of multitemporal airborne laser scanning data and the Fuel Characteristics Classification System for estimating fuel load and consumption. *Journal of Geophysical Research: Biogeosciences*, *127*(5), e2021JG006733.

McKenzie, D., Raymond, C. L., Kellogg, L. K., Norheim, R. A., Andreu, A. G., Bayard, A. C., ... & Elman, E. (2007). Mapping fuels at multiple scales: landscape application of the Fuel Characteristic Classification System. *Canadian Journal of Forest Research*, *37*(12), 2421-2437.

Mell, W., Jenkins, M. A., Gould, J., & Cheney, P. (2007). A physics-based approach to modelling grassland fires. *International Journal of Wildland Fire*, *16*(1), 1-22.

Mell, W. E., Manzello, S. L., Maranghides, A., Butry, D., & Rehm, R. G. (2010). The wildland–urban interface fire problem–current approaches and research needs. *International Journal of Wildland Fire*, *19*(2), 238-251.

Merschel, A. G., Beedlow, P. A., Shaw, D. C., Woodruff, D. R., Lee, E. H., Cline, S. P., ... & Reilly, M. J. (2021). An ecological perspective on living with fire in ponderosa pine forests of Oregon and Washington: resistance, gone but not forgotten. *Trees, Forests and People*, *4*, 100074.

Moran, C. J., Kane, V. R., & Seielstad, C. A. (2020). Mapping forest canopy fuels in the Western United States with LiDAR–Landsat covariance. *Remote Sensing*, *12*(6), 1000.

Nelson Jr, R. M. (2001). Water relations of forest fuels. In *Forest fires* (pp. 79-149). Academic Press.

Nguyen, T. H., Jones, S., Reinke, K. J., & Soto-Berelov, M. (2024). Estimating fine fuel loads in Eucalypt forests using forest inventory data and a modelling approach. *Forest Ecology and Management*, *561*, 121851.

Oliver, William W., and Russell A. Ryker. "Pinus ponderosa Dougl. ex Laws. ponderosa pine." *Silvics of north America* 1.654 (1990): 413.

Ottmar, R. D. (2014). Wildland fire emissions, carbon, and climate: Modeling fuel consumption. *Forest Ecology and Management*, *317*, 41-50.

Ottmar, R. D., Blake, J. I., & Crolly, W. T. (2012). Using fine-scale fuel measurements to assess wildland fuels, potential fire behavior and hazard mitigation treatments in the southeastern USA. *Forest Ecology and Management*, *273*, 1-3.

Ottmar, R. D., Sandberg, D. V., Riccardi, C. L., & Prichard, S. J. (2007). An overview of the fuel characteristic classification system—quantifying, classifying, and creating fuelbeds for resource planning. *Canadian Journal of Forest Research*, *37*(12), 2383-2393.

Ottmar, R. D., Sandberg, D. V., Prichard, S. J., & Riccardi, C. L. (2003a, November). Fuel characteristic classification system. In *Presentation at the 2nd International Wildland Fire Ecology and Fire Management Congress http://ams. confex. com/ams/FIRE2003/techprogram/paper_67236. htm*.

Ottmar, R. D.; Vihnanek, R. E. (1998). Stereo photo series for quantifying natural fuels. Volume II: blackspruce and white spruce types in Alaska. PMS 831. Boise, ID: National Wildfire Coordinating Group, National Interagency Fire Center. 65 p.

Ottmar, R. D.; Vihnanek, R. E. (1999). Stereo photo series for quantifying natural fuels. Volume V: Midwest red and white pine, Northern tallgrass prairie, and mixed oak types in the Central and Lake States. PMS 834. Boise, ID: National Wildfire Coordinating Group, National Interagency Fire Center. 99 p.

Ottmar, R. D.; Vihnanek, R. E. (2000). Stereo photo series for quantifying natural fuels. Volume VI: longleaf pine, pocosin, and marshgrass types in the Southeast United States. PMS 835. Boise, ID: National WildfireCoordinating Group, National Interagency Fire Center. 56 p.

Ottmar, R. D.; Vihnanek, R. E. (2002). Stereo photo series for quantifying natural fuels. Volume IIa: hardwoods with spruce in Alaska. PMS 836. Boise, ID: National Wildfire Coordinating Group, National Interagency Fire Center. 41 p.

Ottmar, R. D.; Vihnanek, R. E.; Mathey, J. W. (2003b). Stereo photo series for quantifying natural fuels. Volume VIa: sand hill, sand pine scrub, and hardwood with white pine types in the Southeast United States with supplemental sites for Volume VI. PMS 838. Boise, ID: National Wildfire Coordinating Group, National Interagency Fire Center. 78 p.

Ottmar, R. D.; Vihnanek, R. E.; Regelbrugge, J. C. (2000a). Stereo photo series for quantifying natural fuels. Volume IV: pinyon-juniper, sagebrush, and chaparral types in the Southwestern United States. PMS 833. Boise, ID: National Wildfire Coordinating Group, National Interagency Fire Center. 97 p.

Ottmar, R. D.; Vihnanek, R. E.; Wright, C. S. (1998). Stereo photo series for quantifying natural fuels. Volume I: mixed-conifer with mortality, western juniper, sagebrush, and grassland types in the Interior Pacific Northwest. PMS 830. Boise, ID: National Wildfire Coordinating Group, National Interagency Fire Center. 73 p.

Ottmar, R. D.; Vihnanek, R. E.; Wright, C. S. (2000b). Stereo photo series for quantifying natural fuels. Volume III: lodgepole pine, quaking aspen, and gambel oak types in the Rocky Mountains. PMS 832. Boise, ID: National Wildfire Coordinating Group, National Interagency Fire Center. 85 p

Ottmar, R. D.; Vihnanek, R. E.; Wright, C. S. (2002). Stereo photo series for quantifying natural fuels. Volume Va: jack pine in the Lake States. PMS 837. Boise, ID: National Wildfire Coordinating Group, National Interagency Fire Center. 49 p.

Pence, M., & Zimmerman, T. (2011). The Wildland Fire Decision Support System: integrating science, technology, and fire management. *Fire Management Today. 71 (1): 18-22.*, 18-22.

Peterson, S. H., Roberts, D. A., & Dennison, P. E. (2008). Mapping live fuel moisture with MODIS data: A multiple regression approach. *Remote Sensing of Environment*, *112*(12), 4272-4284.

Pierce, K. B., Ohmann, J. L., Wimberly, M. C., Gregory, M. J., & Fried, J. S. (2009). Mapping wildland fuels and forest structure for land management: a comparison of nearest neighbor imputation and other methods. *Canadian Journal of Forest Research*, *39*(10), 1901-1916.

Pimont, F., Dupuy, J. L., Rigolot, E., Prat, V., & Piboule, A. (2015). Estimating leaf bulk density distribution in a tree canopy using terrestrial LiDAR and a straightforward calibration procedure. *Remote Sensing*, *7*(6), 7995-8018.

Price, S. J., & Germino, M. J. (2022). Modeling of fire spread in sagebrush steppe using FARSITE: an approach to improving input data and simulation accuracy. *Fire Ecology*, *18*(1), 23.

Prichard, S. J., Kennedy, M. C., Andreu, A. G., Eagle, P. C., French, N. H., & Billmire, M. (2019). Next-generation biomass mapping for regional emissions and carbon inventories: Incorporating uncertainty in wildland fuel characterization. *Journal of Geophysical Research: Biogeosciences*, *124*(12), 3699-3716.

Prichard, S. J., Rowell, E. M., Hudak, A. T., Keane, R. E., Loudermilk, E. L., Lutes, D. C., ... & Hornsby, B. S. (2022). Fuels and consumption. In *Wildland Fire Smoke in the United States: A Scientific Assessment* (pp. 11-49). Cham: Springer International Publishing.

PRISM Climate Group, Oregon State University, https://prism.oregonstate.edu, data created 1 Jan 2021, accessed 1 Jul 2024

QGIS Development Team (2023). QGIS Geographic Information System. Open Source Geospatial Foundation Project.

R Core Team (2022). R: A language and environment for statistical computing. R Foundation for Statistical Computing, Vienna, Austria. URL https://www.R-project.org/.

R Core Team (2023). R: A language and environment for statistical computing. R Foundation for Statistical Computing, Vienna, Austria. URL https://www.R-project.org/.

Rapp, C., Rabung, E., Wilson, R., & Toman, E. (2020). Wildfire decision support tools: An exploratory study of use in the United States. *International journal of wildland fire*, *29*(7), 581-594.

Reeves, M. C., Ryan, K. C., Rollins, M. G., & Thompson, T. G. (2009). Spatial fuel data products of the LANDFIRE project. *International Journal of Wildland Fire*, *18*(3), 250-267.

Reinhardt, E. D. (2003). The fire and fuels extension to the forest vegetation simulator. United States Department of Agriculture, Forest Service, Rocky Mountain Research Station.

Reinhardt, E., Scott, J., Gray, K., & Keane, R. (2006). Estimating canopy fuel characteristics in five conifer stands in the western United States using tree and stand measurements. *Canadian Journal of Forest Research*, *36*(11), 2803-2814.

Riccardi, C. L., Ottmar, R. D., Sandberg, D. V., Andreu, A., Elman, E., Kopper, K., & Long, J. (2007a). The fuelbed: a key element of the Fuel Characteristic Classification System. *Canadian Journal of Forest Research*, *37*(12), 2394-2412.

Riccardi, C. L., Prichard, S. J., Sandberg, D. V., & Ottmar, R. D. (2007b). Quantifying physical characteristics of wildland fuels using the Fuel Characteristic Classification System. *Canadian Journal of Forest Research*, *37*(12), 2413-2420.

Riley, K. L., Grenfell, I. C., Finney, M. A., & Wiener, J. M. (2021). TreeMap, a tree-level model of conterminous US forests circa 2014 produced by imputation of FIA plot data. *Scientific Data*, *8*(1), 11.

Riley, K. L., Grenfell, I. C., Shaw, J. D., & Finney, M. A. (2022). TreeMap 2016 dataset generates CONUS-wide maps of forest characteristics including live basal area, aboveground carbon, and number of trees per acre. *Journal of Forestry*, *120*(6), 607-632.

Riley, K. L., Thompson, M. P., Scott, J. H., & Gilbertson-Day, J. W. (2018). A model-based framework to evaluate alternative wildfire suppression strategies. *Resources*, *7*(1), 4.

Rollins, M. G. (2009). LANDFIRE: a nationally consistent vegetation, wildland fire, and fuel assessment. *International Journal of Wildland Fire*, *18*(3), 235-249.

Rollins, M. G., Keane, R. E., & Parsons, R. A. (2004). Mapping fuels and fire regimes using remote sensing, ecosystem simulation, and gradient modeling. *Ecological Applications*, *14*(1), 75-95.

Rothermel, R. C. (1972). *A mathematical model for predicting fire spread in wildland fuels* (Vol. 115). Intermountain Forest & Range Experiment Station, Forest Service, US Department of Agriculture.

Rothermel, R.C., (1991). *Predicting behavior and size of crown fires in the Northern Rocky Mountains* (Vol. 438). US Department of Agriculture, Forest Service, Intermountain Forest and Range Experiment Station.

Rowell, E., Loudermilk, E. L., Hawley, C., Pokswinski, S., Seielstad, C., Queen, L., ... & Hiers, J. K. (2020). Coupling terrestrial laser scanning with 3D fuel biomass sampling for advancing wildland fuels characterization. *Forest Ecology and Management*, *462*, 117945.

Ruiz-González, A. D., & Álvarez-González, J. G. (2011). Canopy bulk density and canopy base height equations for assessing crown fire hazard in Pinus radiata plantations. *Canadian Journal of Forest Research*, *41*(4), 839-850.

Ryan, K. C., & Opperman, T. S. (2013). LANDFIRE–A national vegetation/fuels data base for use in fuels treatment, restoration, and suppression planning. *Forest Ecology and Management*, *294*, 208-216.

Salajanu, D., & Olson, C. E. (2001). The significance of spatial resolution: Identifying forest cover from satellite data. *Journal of forestry*, *99*(6), 32-38.

Sandberg, D. V., Ottmar, R. D., & Cushon, G. H. (2001). Characterizing fuels in the 21st century. *International Journal of Wildland Fire*, *10*(4), 381-387.

Scott, J. H., & Reinhardt, E. D. (2001). *Assessing crown fire potential by linking models of surface and crown fire behavior* (No. 29). US Department of Agriculture, Forest Service, Rocky Mountain Research Station.

Scott, J. H., & Burgan, R. E. (2005). *Standard fire behavior fuel models: a comprehensive set for use with Rothermel's surface fire spread model*. US Department of Agriculture, Forest Service, Rocky Mountain Research Station.

Shaik, R. U., Fusilli, L., & Giovanni, L. (2021, July). New approach of sample generation and classification for wildfire fuel mapping on hyperspectral (prisma) image. In *2021 IEEE International Geoscience and Remote Sensing Symposium IGARSS* (pp. 5417-5420). IEEE.

Siegert, C. M., Limpert, K. E., Drotar, N. A., Siegle-Gaither, M. L., Burton, M., Lowery, J. A., & Alexander, H. D. (2020, July). Effects of canopy structure on water cycling: Implications for changing forest composition. In *Proceedings of the 20th biennial southern silvicultural research conference. e–Gen. Tech. Rep. SRS–253. US Department of Agriculture, Forest Service, Southern Research Station* (pp. 214-220).

Sikkink, P. G., & Keane, R. E. (2008). A comparison of five sampling techniques to estimate surface fuel loading in montane forests. *International Journal of Wildland Fire*, *17*(3), 363-379.

Sîrbu, I., Benedek, A. M., & Sîrbu, M. (2021). Variation partitioning in double-constrained multivariate analyses: linking communities, environment, space, functional traits, and ecological niches. *Oecologia*, *197*(1), 43-59.

Smith, C. W., Panda, S. K., Bhatt, U. S., Meyer, F. J., & Haan, R. W. (2020, September). Improved Vegetation and Wildfire Fuel Type Mapping Using NASA AVIRIS-NG Hyperspectral Data, Interior AK. In *IGARSS 2020-2020 IEEE International Geoscience and Remote Sensing Symposium* (pp. 1307-1310). IEEE.

Sprintsin, M., Karnieli, A., Berliner, P., Rotenberg, E., Yakir, D., & Cohen, S. (2007). The effect of spatial resolution on the accuracy of leaf area index estimation for a forest planted in the desert transition zone. *Remote Sensing of Environment*, *109*(4), 416-428.

Stefanidou, A., Z. Gitas, I., Korhonen, L., Georgopoulos, N., & Stavrakoudis, D. (2020). Multispectral lidar-based estimation of surface fuel load in a dense coniferous forest. *Remote Sensing*, *12*(20), 3333.

Stephens, S. L., McIver, J. D., Boerner, R. E., Fettig, C. J., Fontaine, J. B., Hartsough, B. R., ... & Schwilk, D. W. (2012). The effects of forest fuel-reduction treatments in the United States. *BioScience*, *62*(6), 549-560.

Stevens-Rumann, C. S., Hudak, A. T., Morgan, P., Arnold, A., & Strand, E. K. (2020). Fuel dynamics following wildfire in US Northern Rockies forests. *Frontiers in Forests and Global Change*, *3*, 51.

Stovall, A. E., & Atkins, J. W. (2021). Assessing low-cost terrestrial laser scanners for deriving forest structure parameters.

Szpakowski, D. M., & Jensen, J. L. (2019). A review of the applications of remote sensing in fire ecology. *Remote sensing*, *11*(22), 2638.

Theobald, D. M., & Romme, W. H. (2007). Expansion of the US wildland–urban interface. *Landscape and Urban Planning*, *83*(4), 340-354.

Thompson, M. P., & Calkin, D. E. (2011). Uncertainty and risk in wildland fire management: a review. *Journal of environmental management*, *92*(8), 1895-1909.

Thompson, M. P., Vogler, K. C., Scott, J. H., & Miller, C. (2022). Comparing risk-based fuel treatment prioritization with alternative strategies for enhancing protection and resource management objectives. *Fire Ecology*, *18*(1), 26.

Tinkham, W. T., Hoffman, C. M., Canfield, J. M., Vakili, E., & Reich, R. M. (2015). Using the photoload technique with double sampling to improve surface fuel loading estimates. *International Journal of Wildland Fire*, *25*(2), 224-228.

Tinkham, W.T., Mahoney, P.R., Hudak, A.T., Domke, G.M., Falkowski, M.J., Woodall, C.W., Smith, A.M.S. (2018). Applications of the United States forest inventory and analysis dataset: a review and future directions. *Canadian Journal of Forest Research*, *48*(11), 1251-1268.

USDA Forest Service. (2022). “Confronting the Wildfire Crisis: A Strategy for Protecting Communities and Improving Resilience in America’s Forests.

USFS. Phase 3 field guide to the down woody material inventory. (2018).

Vakili, E., Hoffman, C. M., & Keane, R. E. (2016). Fine woody fuel particle diameters for improved planar intersect fuel loading estimates in Southern Rocky Mountain ponderosa pine forests. *International Journal of Wildland Fire*, *25*(7), 780-784.

Vaillant, N. M., & Reinhardt, E. D. (2017). An evaluation of the Forest Service Hazardous Fuels Treatment Program—Are we treating enough to promote resiliency or reduce hazard?. *Journal of Forestry*, *115*(4), 300-308.

Varner, J. M., Hiers, J. K., Ottmar, R. D., Gordon, D. R., Putz, F. E., & Wade, D. D. (2007). Overstory tree mortality resulting from reintroducing fire to long-unburned longleaf pine forests: the importance of duff moisture. *Canadian Journal of Forest Research*, *37*(8), 1349-1358.

Vogeler, J. C., Yang, Z., & Cohen, W. B. (2016). Mapping post-fire habitat characteristics through the fusion of remote sensing tools. *Remote Sensing of Environment*, *173*, 294-303.

Volkova, L., Sullivan, A. L., Roxburgh, S. H., & Weston, C. J. (2016). Visual assessments of fuel loads are poorly related to destructively sampled fuel loads in eucalypt forests. *International Journal of Wildland Fire*, *25*(11), 1193-1201.

Waddell, K. L. (2002). Sampling coarse woody debris for multiple attributes in extensive resource inventories. *Ecological indicators*, *1*(3), 139-153.

Wagner, C. V. (1977). Conditions for the start and spread of crown fire. Canadian Journal of Forest Research, 7(1), 23-34.

Walker, S. M., Murray, L., & Tepe, T. (2016). Allometric equation evaluation guidance document. *Winrock International, USA*.

Wooster, M. J., Roberts, G. J., Giglio, L., Roy, D. P., Freeborn, P. H., Boschetti, L., ... & San-Miguel-Ayanz, J. (2021). Satellite remote sensing of active fires: History and current status, applications and future requirements. *Remote Sensing of Environment*, *267*, 112694.

Wright, C. S.; Ottmar, R. D.; Vihnanek, R. E.; Weise, D. R. (2002). Stereo photo series for quantifying natural fuels. Grassland, shrubland, woodland, and forest types in Hawaii. Gen. Tech Rep. PNW-GTR-545. Portland, OR: U.S. Department of Agriculture, Forest Service, Pacific Northwest Research Station. 91 p.

Yung-Han, H., Chen, Y., Yang, T.-R., Kershaw, J.A., Ducey, M. J. (2020). Sample strategies for bias correction of regional LiDAR-assisted forest inventory estimates on small woodlots. *Annals of Forest Science, 77*, 75.

Ziegler, J. (2014). *Impacts of treatments on forest structure and fire behavior in dry western forests* (Master's thesis, Colorado State University).